PL-TR-91-2135

REGIONAL-SCALE ANALYSIS AND FORECASTING (RAP) REPORT

John C. Burgeson
Christopher R. Redder
Isidore M. Halberstam
Ralph Shapiro

Science and Technology Corporation
P.O.Box 7390
Hampton, VA 23666

May 1991

Scientific Report No. 1

PHILLIPS LABORATORY
AIR FORCE SYSTEMS COMMAND
HANSCOM AIR FORCE BASE, MASSACHUSETTS 01731-5000

"This technical report has been reviewed and is approved for publication"

HENRY A. BROWN
Contract Manager
Atmospheric Structure Branch

DONALD D. GRANTHAM, Chief
Atmospheric Structure Branch
Atmospheric Sciences Division

FOR THE COMMANDER

DONALD A. CHISHOLM, Acting Director
Atmospheric Sciences Division

This report has been reviewed by the ESD Public Affairs Office (PA) and is releasable to the National Technical Information Service (NTIS).

Qualified requestors may obtain additional copies from the Defense Technical Information Center.

If your address has changed, or if you wish to be removed from the mailing list, or if the addressee is no longer employed by your organization, please notify PL/IMA, Hanscom AFB, MA 01731. This will assist us in maintaining a current mailing list.

Do not return copies of this report unless contractual obligations or notices on a specific document requires that it be returned.

REPORT DOCUMENTATION PAGE

Form Approved
OMB No 0704-0188

1. AGENCY USE ONLY (Leave blank)	2. REPORT DATE	3. REPORT TYPE AND DATES COVERED
	May 1991	Scientific Report No. 1

4. TITLE AND SUBTITLE
Regional-Scale Analysis and Forecasting (RAP) Report

5. FUNDING NUMBERS
PE 63707F
PR 2688 TA 01 WU JC

Contract F19628-89-C-0167

6. AUTHOR(S)
John C. Burgeson
Christopher R. Redder
Isidore M. Halberstam*
Ralph Shapiro*

7. PERFORMING ORGANIZATION NAME(S) AND ADDRESS(ES)
Science and Technology Corporation
P.O. Box 7390
Hampton, VA 23666

8. PERFORMING ORGANIZATION REPORT NUMBER

9. SPONSORING / MONITORING AGENCY NAME(S) AND ADDRESS(ES)
Phillips Laboratory
Hanscom AFB, MA 01731-5000

Contract Manager: H.A. Brown/LYA

10. SPONSORING / MONITORING AGENCY REPORT NUMBER
PL-TR-91-2135

11. SUPPLEMENTARY NOTES
*STX Corporation

12a. DISTRIBUTION / AVAILABILITY STATEMENT
Approved for public release;
Distribution unlimited

12b. DISTRIBUTION CODE

13. ABSTRACT *(Maximum 200 words)*

This interim report describes the development of the RAP at the halfway point of the contracted effort. The RAP is based on optimum interpolation and rigorous selection by forward stepwise regression of a small subset of the observations available for interpolation to a point. The RAP scheme produces analyses that are nearly as accurate as analyses produced by interpolating the full set of observations to the point. Another unique feature of the RAP is a buddy check that very carefully determines those observations that should be eliminated from affecting the analysis. The scheme used simulated error correlations, which were a function of distance between observations, but will be using error correlation models developed from real data. The correlation models will be stratified by region, season, standard atmospheric levels, forecast lengths, and sensors. The RAP will be used in observing system simulation experiments (OSSEs). The simulated observations will be obtained from "perfect" FGGE-2b databases after insertion of observation errors. The "perfect" FGGE-2b observations were derived from a 16-day nature forecast run from the ECMWF. The OSSEs will be used to determine the goodness of RAP and the validity of the developed correlation models.

14. SUBJECT TERMS	15. NUMBER OF PAGES
Optimum interpolation, stepwise regression, forecast error correlations, observation system simulation experiments, numerical weather analysis, numerical weather forecast models, and databases.	86
	16. PRICE CODE

17. SECURITY CLASSIFICATION OF REPORT	18. SECURITY CLASSIFICATION OF THIS PAGE	19. SECURITY CLASSIFICATION OF ABSTRACT	20. LIMITATION OF ABSTRACT
Unclassified	Unclassified	Unclassified	SAR

TABLE OF CONTENTS

LIST OF FIGURES

LIST OF TABLES

FOREWORD

Science and Technology Corporation (STC) is pleased to submit this interim report entitled "Regional-scale Analysis and Forecasting (RAP) Report" as part of Contract No. F19628-89-C-0167. The long-term objective is to develop and demonstrate a regional analysis procedure (RAP) using optimum interpolation (OI) in both real and simulation modes. The RAP will assimilate all available meteorological data and fuse it efficiently into a high resolution analysis of mass, motion, and moisture fields. This report describes the five major tasks to be accomplished, the present status of those tasks, the optimum interpolation scheme, the development of the RAP databases, case studies of experiments in numerical analysis, and plans for completing the major tasks. The valuable technical assistance provided by Donald Norquist, Contract Monitor, is acknowledged and greatly appreciated.

1. INTRODUCTION

The foundation of the relocatable regional analysis procedure (RAP) has been solidly established. RAP is a multivariate, multisource analysis scheme for relocatable, regional-scale applications. Specifically, the scheme incorporates optimum interpolation for the numerical analysis and stepwise regression for selection of observations.

The procedure uses meteorological fields from various sources on a regional scale analysis grid, called uniform gridded data fields. Observations of varying availability in time and space are used in an optimum sense to produce the best possible depiction of the variables within the regional atmospheric volume.

In addition, observing system simulation experiments will be conducted to establish confidence levels for the regional analyses. Finally, various short term (out to 12 hr) regional forecast methods (such as persistence, numerical or some combination) will be examined for the purpose of recommending an optimal forecast procedure.

A brief description of present RAP objectives is provided below. The remainder of the report describes the five major tasks to be accomplished, the present status of those tasks, the optimum interpolation scheme, the development of the RAP databases, case studies of experiments in numerical analysis, and plans for completing the major tasks.

The long-term objective of the RAP is to develop and demonstrate a regional analysis procedure using optimum interpolation (OI) in both real and simulation modes. The RAP will assimilate all available meteorological data and fuse them efficiently into a high resolution analysis of mass, motion, and moisture fields. To accomplish the long-term objective, several short-term objectives are presently being pursued:

1. Restructuring the observations database so that forecast errors can be calculated efficiently

2. Performing numerical analysis experiments with the observation and forecast database to test the multivariate optimum interpolation scheme in all analysis variables, ensuring that the resulting analyses are dynamically consistent

3. Completing the calculation of error statistics (differences between the Relocatable Window Forecast Model [RWFM] forecasts and observations) and developing error correlation functions

4. Continuing to integrate into the RAP the latest techniques obtained from the literature on developing operational optimum interpolation schemes and specifying the errors of present and future observing systems

5. Completing the extraction of the First GARP (Global Atmospheric Research Program) Global Experiment (FGGE)-2b observations and T-106 nature run forecasts from magnetic tapes from the European Center for Medium Range Weather Forecasts (ECMWF), and unpacking the required gridded forecast fields that can be interpolated to the observation points to simulate an observation network for use in observing systems simulation experiments (OSSEs)

6. Generating RWFM forecasts from the nature run

7. Testing the RWFM verification model (RWFMVER)

2. RAP TASKS

The research and development effort, which requires a great deal of software modification and development, is specified in the Science and Technology Corporation (STC) Technical Report 3072, RAP Initial Work Plan, September 1989. Each of the five dependent tasks and a brief summary of the progress toward their completion are described. STC Task 4, which was begun most recently, is described in considerable detail. Appendix A is a report on the software modification and development required for RAP.

2.1 STC Task 1

Task 1 is to develop an automated relocatable, regional multivariate objective analysis procedure using optimum interpolation (OI). There are two major subtasks: (1) design and develop an OI scheme, and (2) incorporate the RAP analysis algorithm into the relocatability and variable resolution framework of the Relocatable Window Analysis Model (RWAM).

The OI scheme, based on objective data selection and buddy checking by forward stepwise regression (FSR), has now been carefully tested on all meteorological variables, specifically, surface pressure, height of isobaric levels, temperature, humidity, and u-wind and v-wind components.

The RWAM is presently in a nonoperational status at the Air Force Global Weather Central (AFGWC), which has not delivered the RWAM code (and probably will not in the near term); therefore, work was focused on completing the testing of the OI scheme.

2.2 STC TASK 2

Task 2 also has two subtasks. The primary subtask is to compute and model the first-guess forecast errors, from which correlation functions can be developed to model these errors. The secondary subtask is to determine and model observation errors, if these are needed by the OI scheme.

The primary task has dominated much of the effort so far, requiring first the development of extensive analysis, forecast, and observations databases, which are ready for use. The module that calculates error correlations is based on Hollingsworth and Lonnberg (1986), Lonnberg and Hollingsworth (1986), and Thiebaux et al. (1986). The design (Section 4.5) specifies that the correlation pairs will be placed into bins, which are a function of the distance between the pairs, and averaged.

As shown in Section 3.1, the theory of the OI scheme leads to the conclusion that the observation errors are of secondary importance. The small errors in the case studies of numerical analyses, discussed in Section 5, indicated that the conclusion is true. Nevertheless, this assertion remains to be proved.

2.3 STC TASK 3

Task 3 is to develop a relocatable verification package, using standard measures of error such as the RWFM verification model (RWFMVER), the Phillips Laboratory (PL) Global Spectral Model (GSM) diagnostic package, and map comparisons. The package is for testing RAP formally in real data experiments. This testing will include comparing RAP against RWAM, the AFGWC High-Resolution Analysis Model (HIRAS), and real observations, and with forecasts made by the AFGWC Relocatable Window Forecast Model and the PL GSM.

The forecast comparisons have been completed, and RWFMVER is presently being converted to execute on the RAP automated data processing system. Under this task RAP will be run on scenarios not included in the original database, and RAP will be checked against other analyses and observations. Also, the verification package can be used to improve RAP's methodology.

2.4 STC TASK 4

The observing systems simulation experiments (OSSEs) can proceed formally only after demonstrated success of Tasks 1 and 2 in Task 3. The OSSEs consist of several subtasks, all of which will require 2 years to complete. They are described in detail because they will be the main focus of effort for the remainder of this project.

1. The first subtask, to build a database of simulated FGGE-2b observations from the ECMWF T-106 nature run tapes, is partially completed. The ECMWF GRIB software was used to extract selected forecast files from the tapes at the Phillips Laboratory/Geophysics Directorate (PL/GP) Computer Center. In addition, the FGGE-2b files have also been extracted. All required files (forecasts and upper air observations at 6-hr intervals from 19 January 1979 through 1 February 1979) have been transferred to the CRAY-2 at the Phillips Lab Supercomputer Center (PLSC), where the needed fields will be unpacked and stored on a 1x1 degree grid at mandatory levels. "Perfect" observation files at FGGE-2b data locations will be simulated by interpolating the forecasts from the grid to the observation points to replace data actually observed.

The following detailed description of the plans for the OSSEs is in three parts that follow one after the other in natural sequence: the development of datasets of "perfect observations," the development of an analysis and forecast database, and the preparation of RAP analyses under different scenarios.

The next step is to simulate an observation network of existing and proposed sensors/systems by interpolating the gridded T-106 forecast data to FGGE-2b observation points to mimic "real" data tapes. By assigning errors (random and systematic instrument errors) to these "observations" extracted from the nature run, we can create files of simulated observations.

The Air Force Geophysics Laboratory (AFGL) Statistical Analysis Package (ASAP), which takes a 1x1 gridded first guess field and interpolates it to observation points, has been modified to accept T-106 gridded data. Perfect FGGE-2b files will be built by treating each gridded nature run field as a first guess, modifying the MASTORX subroutines to read the FGGE-2b observations from the files, and writing an output file with the corresponding nature run values at each site.

Software is being developed to generate "perfect observations" by ingesting and time-interpolating the T-106 "nature run" ontime forecasts (at 00, 06, 12, and 18 UTC) to FGGE-2b observation points, including satellite data and AIREPS. A second set of data, developed by introducing desired observational (random and correlated) errors, will be used to act as the actual simulated FGGE-2b observations at 6-hr intervals.

2. The second major subtask is to generate an analysis and forecast database from the simulated FGGE-2b observations. The database will make up the CONTROL scenario, which is based on the existing observation system, for the RAP OSSEs. The procedure is described below and depicted in Fig. 1 on pages 6 and 7.

First, 3-day global "spin-up" atmospheres are generated by running GSM forecasts for 72 hr, initialized at 00 UTC on 16, 21, and 26 January 1979 with the nature run from the ECMWF to ensure there are ample differences between the nature run and analyses. Next, ASAP begins with each of the 72 hr GSM forecasts and produces the

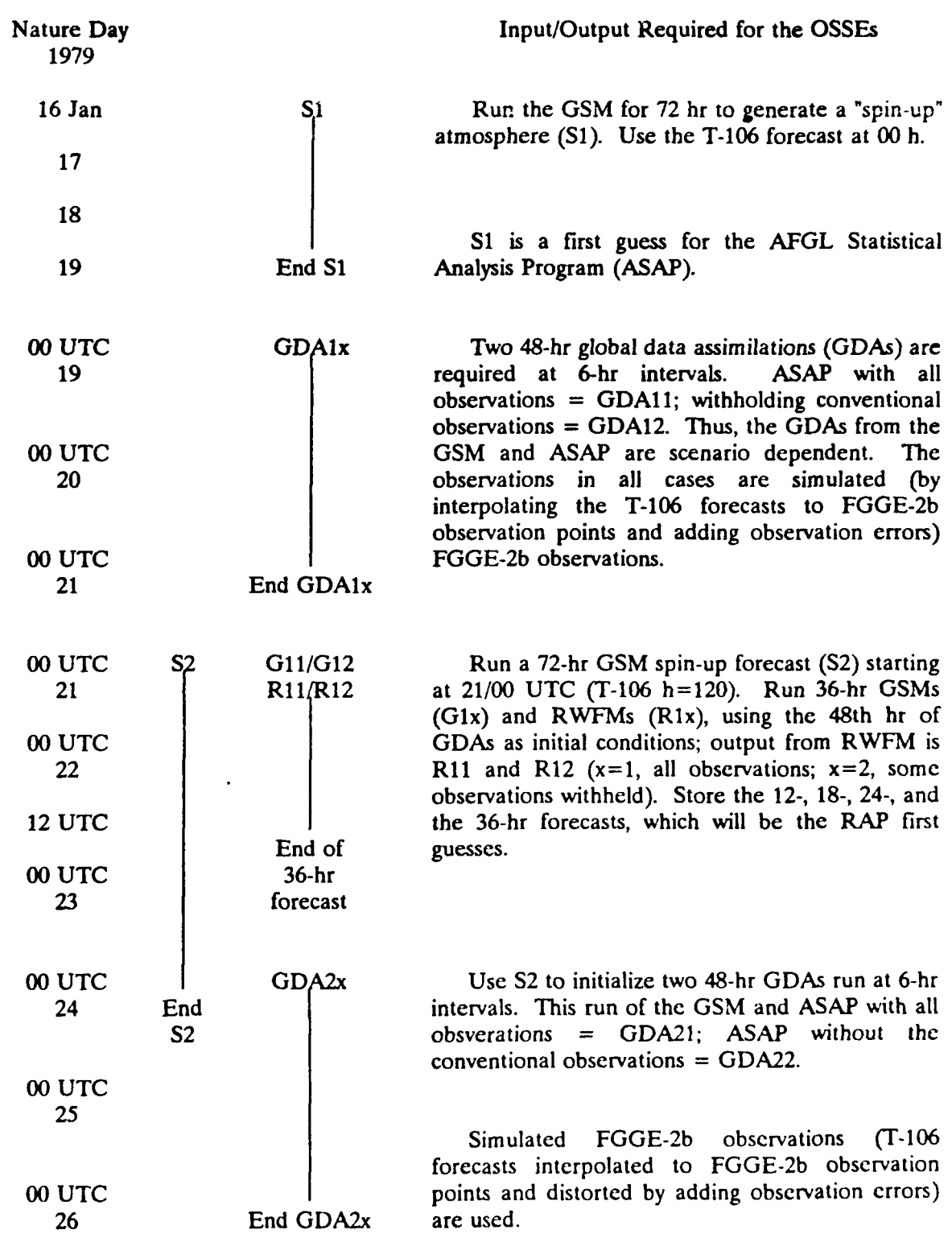

Figure 1. A depiction of the process for generating the OSSE databases.

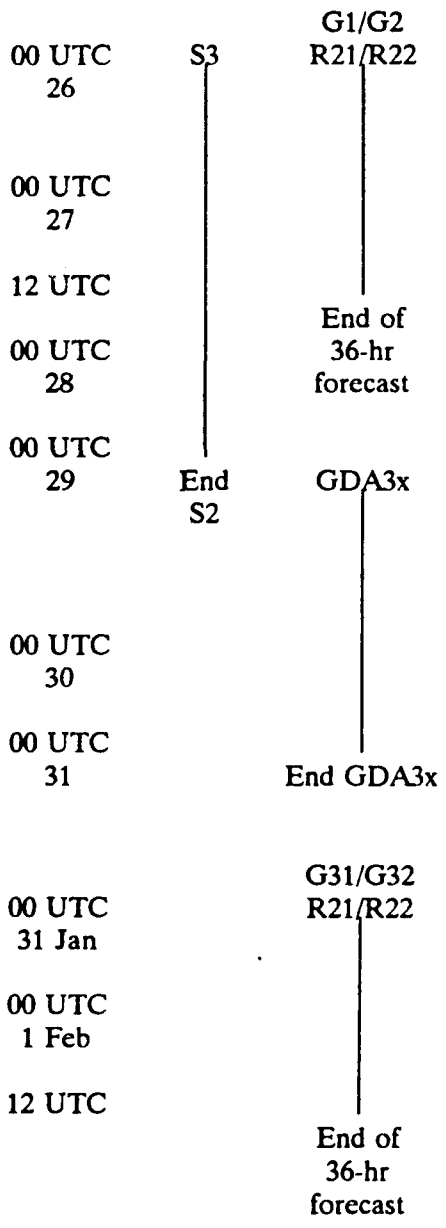

Run the third 72-hr GSM spin-up forecast (S3), starting at 26/00 UTC, that is, T-106 forecast h=240. Start the 2nd run 36-hr GSMs (G2x) and RWFMs (R2x), using the 48th hr of GDAs as initial conditions; output from RWFM is R21 and R22, which will be 1st guesses for RAP.

Store the 12-, 18-, 24-, and 36-hr forecasts.

Recall that x=1 implies that all the FGGE-2b simulated observations will be used; x=2 implies that conventional observation points will be withheld.

Use S3 to initialize the third (and final) set of two 48-hr GDAs at 29/00 UTC and run at 6-hr intervals. Define the GSM/ASAP with all observations = GDA31; the ASAP without the conventional observations = GDA32.

The observations are, of course, (the T-106 forecasts interpolated to FGGE-2b observation points, where the observation errors are added) the simulated FGGE-2b observations.

Start the third (and final) 36-hr GSM forecasts (G3x) and RWFMs (R3x), where x=1 for all observations and x=2 for withheld observations. Use the 48th hr of GDA3x as initial conditions; output from RWFMs is R31 and R32, which will be first guesses for RAP.

Store the 12-, 18-, 24-, and 36-hr forecasts for RAP first guesses.

Figure 1. (Concluded) A depiction of the process for generating the OSSE databases.

GSM forecasts, one with conventional (that is, RAOB, PIBAL, and AIREPS) observations and one without conventional observations in a hostile zone (that is, using only satellite data in that specific volume).

RWFM forecasts (which begin at 00 UCT on 21, 26, and 31 January 1979 of the nature run) will be generated from the GDAs. The GDAs are input to the GSM, 2-day global data assimilations (GDAs) using the globally simulated FGGE-2b observations at 6-hr cycles. There will be two GDAs for each of the three 72-hrwhich will be run for 36 hr to provide 6-hr forecast fields. These fields are the initial and boundary conditions for 36-hr runs of the RWFM for the Eurasian and the Central American regions.

RWFMVER will be used to compare RWFM forecasts (filtered to the nature grid) with the nature run. The purpose is to determine the RWFM forecast errors as a function of region and forecast length, and compare simulation errors with actual forecast errors (from Task 2) to assess the realism of the OSSEs.

3. The final step is to prepare several RAP analyses from the simulated databases and access the value of the experiments. With RWFM forecasts valid at 12, 18, 24, and 36 hr, and 12-hr- and 24-hr-old RAP analyses as the first guess, RAP will generate analyses using the requested scenarios of simulated observations (Schaaf, 1990), that is,

- CONTROL: existing observing system
- ALLOBS: existing and proposed observations systems
- TACOBS: ALLOBS except TOVS and conventional observations in hostile side of battle area, but in "HIRAS" exclude only the conventional observations
- OLDOBS: (1) 12-hr RWFM forecast valid at time t and offtime observations at t-6 hr
  (2) same as (1) but with 24-hr RWFM forecast
  (3) 18-hr RWFM forecast at time t+6 and ontime observations at time t

RWFMVER will be used to compare (grid-to-station and grid-to-grid) RAP analyses, which are filtered to the nature grid ("truth" for the OSSEs), with the Nature Run. Comparisons are required with RWFM, RWAM (if available), and GSM for each

region at the above time periods and data denial scenarios. Also, analysis errors (computed as a by-product of OI) will be compared with RAP-nature differences to determine the real forecast error statistics generated for the error-level module in Task 2, and they will be tabulated by region, season, first guess scenario, and data denial scenario.

2.5 STC TASK 5

Survey the literature for candidate forecast techniques to extend the RAP analysis out to 12 hr. The obvious candidate, persistence, may not be a good 12-hr forecast for small regions because of advection. STC will consider both dynamical and statistical techniques; for example, the known difference field between the RAP and the RWFM 00-hr forecast could be used to modify the RWFM 12-hr forecast. STC will document the advantages and disadvantages of techniques for use in the field and recommend a candidate for further study.

3. THEORETICAL AND PRACTICAL CONSIDERATIONS OF OPTIMUM INTERPOLATION

Optimum interpolation, also known as statistical interpolation, was selected as the analysis scheme for the RAP. The following subsections discuss the details of the scheme and the rationale for our technical approach, in particular, the methodology for rigorously selecting observations and the modeling of correlation structure functions.

3.1 SENSITIVITY OF INTERPOLATION WEIGHTS TO CORRELATION FUNCTIONS

Given a gridpoint (g) surrounded by a number of observation points, i, (i = 1, 2, . . ., n), the process of optimum interpolation determines the relative weights (W_i) assigned to each observation in the expression,

$$f_g^A = f_g^P + \sum_{i=1}^{N'} W_i (f_i^O - f_i^P) \qquad (1)$$

where f_g is the estimated (or analyzed) value of the variable at the gridpoint g, f_g^P is a preliminary (first guess) value of the variable at g, and f_i^O and f_i^P are respectively, observed and first guess values of the variable at the observation points. In Eq. 1, $N' \leq N$, implies that it may be desirable

to use fewer than all of the available observations. Since, in general, first guess values are obtained from a prior prediction of the field quantity, (f), f^p is generally available only at gridpoints of the prediction model, that is f^p_g. Therefore, the f^p_i are obtained by a suitable interpolation process from the f_g.

Keegan and Shapiro (1985) showed that the consistent, as well as the simplest, system of equations to use in obtaining the weights W_i in Eq. 1, is their Eqs. 2-16. That is,

$$\sum_{i=1}^{N'} W_i r(\Delta_i, \Delta_j)\, \sigma_{\Delta_i} \sigma_{\Delta_j} = r(\Delta_j, \Delta_g)\, \sigma_{\Delta_j} \sigma_{\Delta_g} + r(\Delta_j, \epsilon^o_g)\, \sigma_{\Delta_j} \sigma_{\epsilon^o_g} \qquad (2)$$

where $j = 1, 2, \ldots, N'$ also indicates an observation point, r(a, b) is the linear correlation coefficient between the parameters a and b, σ_a is the standard deviation of a, $\Delta_i = f^p_i - f^o_i$ and $\epsilon^o_g = f^o_g - f_g$ indicates the deviation of the observed value of the variable at the gridpoint (f^o_g) from the true value (f_g). In other words, ϵ^o_g is the observation error at the gridpoint and is an unknown quantity since the true value of the variable f is unknown everywhere (both at gridpoints and observation points) and the observed value f^o_g must be obtained by interpolation from f^o_r. Since ϵ^o_g in Eq. 2 enters as a correlation with Δ_j, it is likely that $r(\Delta_j,\epsilon_g) << r(\Delta_j,\Delta_g)$. Therefore, neglect $r(\Delta j,\epsilon^o_g)$, and the right-hand side of Eq. 2 contains only the first term $r(\Delta_j,\Delta_g)\sigma_{\Delta_j}$. (The significance of this assumption will be tested in the simulation mode by assigning a series of nonzero values to the neglected correlation and re-evaluating the W_r.) Note that $\Delta_g = f^p_g - f^o_g$ implies that an estimate of the observed value at the gridpoint must be obtained by a suitable interpolation process from the f^o_r.

The basic problem in the solution of the simplified form of Eq. 2 is the specification of the Δ_i, Δ_j, and Δ_g statistics, namely, $r(\Delta_i, \Delta_j)$, $r(\Delta_i, \Delta_g)$, and σ_i, σ_j, and σ_g. If accurate estimates of these quantities were available, the application of OI would be a simple matter. Unfortunately, the relevant statistics are essentially unknown. While some limited studies have been made on $r(f^o_i, f^o_j)$, the required correlation fields of $r(\Delta_i,\Delta_j)$ are model dependent; therefore, because of the rapid rate of alterations in operational models there has been no possibility of developing long series of both predicted and observed quantities from which the required statistics can be obtained.

In spite of this shortage of data, a substantial literature (e.g., Dey and Morone, 1985; and DiMego, 1988) exists on the advantages and disadvantages of various models of the required

correlation functions. Without a firmer foundation in the facts of observations, however, it is not feasible now to attempt to choose the best from among the various correlation models. STC Task 2 includes preparing a small sample of observational data, which matches forecasts from an operational model, and calculating suitable correlation models and standard deviation statistics. Nevertheless, it was useful first to test the sensitivity of the W_i derived from Eq. 2 to variations in the correlation functions.

Expanding Eq. 2, neglecting $r(\Delta_j, \epsilon_g^o)$, and assuming the data have been normalized so that $\sigma_{\Delta_i} = \sigma_{\Delta_j} = \sigma_{\Delta_g} = 1$, for one gridpoint g and n observation points the following linear equations describe the system.

$$\begin{aligned}
W_1 r_{11} + W_2 r_{21} + \ . \ . \ . \ + W_n r_{n1} &= r_{g1} \\
W_1 r_{12} + W_2 r_{22} + \ . \ . \ . \ + W_n r_{n2} &= r_{g2} \\
\ . \qquad \ . \qquad \ . \qquad \ . \qquad \ . \\
\ . \qquad \ . \qquad \ . \qquad \ . \qquad \ . \\
\ . \qquad \ . \qquad \ . \qquad \ . \qquad \ . \\
W_1 r_{1n} + W_2 r_{2n} + \ . \ . \ . \ + W_n r_{nn} &= r_{gn}
\end{aligned} \tag{3}$$

where, for example, $r_{12} = r(\Delta_1, \Delta_2)$ and $r_{g1} = r(\Delta_1, \Delta_g)$.

It is apparent from Eq. 3 that the W_i are the coefficients of the multiple regression of Δ_g on all the Δ_i, Δ_j. If the various correlations in Eq. 3 were known precisely, the total normalized information content in the n observations with regard to their ability to estimate the analyzed value of the variable at the gridpoint f_g^a would be given by the square of the multiple correlation coefficient. For example, if n = 2 and $r_{g1} = 0.9$, $r_{g2} = 0.8$, and $r_{12} = 0.7$, then the multiple correlation coefficient ($r_{g1,2}$) is 0.9309, $W_1 = 2/3$, $W_2 = 1/3$, and the normalized explained variance is 0.8667. This particular set of correlations implies that observation point 1 is close to gridpoint g and that observation point 2 is somewhat more distant from gridpoint g, but closer to gridpoint g than point 1. On the other hand, with the same distribution of observation points with respect to the gridpoint, but with substantially different correlations ($r_{g1} = 0.7$, $r_{g2} = 0.6$, $r_{12} = 0.5$), the weights are not very different. In this case $W_1 = 0.5333$ instead of 0.6667, but W_2 is still 1/3. Also, the multiple correlation and explained variance are substantially different, namely 0.7572 and 0.5733, respectively. While it is desirable to have multiple correlation coefficients that are near unity,

implying small mean square error, in any one realization most if not the only significance is contained in the weights. Precise modeling of the various correlation functions is probably less important then having simple, but self-consistent modeling functions.

Tests of the sensitivity of the W_i, first in a domain with two observation points and subsequently with increased numbers of observation points suggest that the above hypothesis is true. Assigning correlations as in the preceding examples and covering a complete range of all reasonable correlations offers a study that has the advantage of not being dependent on the availability of real data (observations and model output). Such studies not only provide more definitive answers to questions on the sensitivity of the W_i to the values of the respective correlations, but they also clarify the question of whether to limit the number of observations or to use all available observations. For example, if there are two observations close to each other but somewhat distant from the gridpoint, then $r_{g1} = r_{g2} = 0.7$ and $r_{12} = 0.9$ are reasonable results. In this case, the multiple correlation ($r_{g1,2} = 0.7182$) is not much larger than either bivariate correlation, and the weights are $W_1 = W_2 = 0.3684$. Either observation by itself would contain almost the same information as both together, but the use of both has the advantage of partially suppressing random errors of observation.

Table 1 illustrates the type of information that can be obtained from the sensitivity analysis, even though this partial example contains only two observation points. With r_{g1}, and r_{g2} as given (0.5 and 0.3, respectively), when r_{12} is small (such as when 1 and 2 are on opposite sides of g), say for example, 0, 0.1, and 0.2, the weights are nearly 0.5 and 0.3, respectively. When r_{12} is comparable to r_{g1} and r_{g2} (say 0.3 to 0.7), W_2 is near zero and W_1 is near 0.5. When r_{12} is large($\geq .08$), W_2 is more and more negative as $r_{12} \Rightarrow 1.0$, and W_1 is more and more positive; but the sum of the weights $W_1 + W_2 < 0.45$. With r_{g1} and r_{g2} as given in Table 1, it is not possible for r_{12} to be larger than 0.97; otherwise r_{g1}, and r_{g2} could not differ as much as they do. With $r_{12} \geq 0.98$, the multiple correlation would be greater than 1, and the solution matrix from Eq. 3 would be degenerate (ill-conditioned).

3.2 FINAL SELECTION OF OBSERVATIONS IN OPTIMUM INTERPOLATION

On the basis of some preliminary studies including 26 randomly distributed artificial observations within a regional area as well as follow-on studies involving densely distributed real data

Table 1. Example of a sensitivity analysis, where r_{g1} is the coefficient of correlation between gridpoint g and observation point 1, $r_{g,1,2}$ is the multiple correlation coefficient, and W_1 and W_2 are the relative weights assigned to observations at points 1 and 2, respectively.

r_{g1}	r_{g2}	r_{12}	$r_{g,1,2}$	W_1	W_2
0.5	0.3	0	0.583	0.5000	0.3000
0.5	0.3	0.1	0.560	0.4747	0.2525
0.5	0.3	0.2	0.540	0.4583	0.2083
0.5	0.3	0.3	0.524	0.4505	0.1648
0.5	0.3	0.4	0.512	0.4524	0.1190
0.5	0.3	0.5	0.503	0.4667	0.0667
0.5	0.3	0.6	0.500	0.5000	0.0000
0.5	0.3	0.7	0.505	0.5686	-0.0980
0.5	0.3	0.8	0.527	0.7222	-0.2778
0.5	0.3	0.9	0.607	1.2105	-0.7895
0.5	0.3	0.95	0.751	2.2051	-1.7949
0.5	0.3	0.97	0.911	3.5364	-3.1303

in a European region, the decision was made to base the observation selection procedure on stepwise linear regression. This section discusses the results of these studies and presents a conceptual overview of the nature of stepwise regression. To set the stage some relevant background is provided in the form of several slightly edited pages from Keegan and Shapiro (1985), a report prepared under contract with the U.S. Air Force Geophysics Laboratory (AFGL), which is now Phillips Laboratory.

> The selection of the relevant observations is a complex problem. An analysis volume must first be specified. This is a time-space volume containing the interpolation point and all relevant observations. Since correlations between observations generally decrease with increasing space (distance or time), the analysis volume will probably have a radius approximating the distance corresponding to zero correlation between the relevant parameters, although this need not be strictly true. This volume, however, may incorporate many potential observations of different types, different independent, and different relevancies. The selection system must be able to assign weights to the relevant observations consistent with their independent information content. In essence, the problem of selection of observations may be considered to be a multiple linear regression problem. Equation 2 shows that the correlation between each pair of independent variables as well as between the dependent variable and each of the independent variables may influence the W_i. However,

while some of the operational OI systems resemble a multiple linear regression approach, all depart from such an approach to some extent.

With regard to the selection of observations, it would be desirable to eliminate, as far as possible, the arbitrariness in the OI procedure. If too many observations are allowed to influence the value of the analyzed variable, not only do the computations become laborious, but the analysis error may actually increase. The independent information contributed by each observation generally decreases in proportion to the number of observations, as a result of intercorrelation among the independent variables. (This is the well-known problem of multicolinearity in linear regression, leading to ill-conditioned matrices with small determinants.) On the other hand, if because of arbitrary selection rules, too few observations are selected, the analysis will be far from optimum.

A rational basis for selecting the observations that will be allowed to influence the analyzed value is required. The first step in this selection process is rather simple since it involves the establishment of a two-, three-, or four-dimensional influence space, where any observation has a possibility of affecting the value of the analysand. In a sense, defining an influence space is artificial, since if computational power were great enough, this space might just as well encompass the entire regional atmosphere for the current time as well as some considerable antecedent time period. However, in this case, the second and more difficult part of the data selection problem (discussed below) would be greatly aggravated.

The second part of the problem, the choice of potential observations which will affect the analyzed value, requires substantial investigation. Several investigators have found that the use of four or five parameters is generally sufficient to obtain the best estimate (lowest root mean square errors [RMSE]) for the interpolated value. If a smaller or larger number of observations is allowed to influence the analysand, the error generally increases. Thus, it appears that the number of potential observations should be large, but the number actually selected for the interpolation should be small.

Of course it is possible to avoid the problem of how to select a few "best" observations from many within the influence space, by using virtually all of them. However, as we have already indicated, this too is unlikely to be the best procedure, in terms of both the accuracy and stability of the results as well as in terms of the computational effort involved. Stepwise regression has been used for many years as a possible solution to the selection process in multivariate regression.

While stepwise regression does not guarantee the best selection of "predictors," a large body of experience has demonstrated its effectiveness as a practical regression technique that can approach the "best" solution when properly applied. Stepwise regression avoids the arbitrary limitation and selection procedure of the National Meteorological Center (see Hoke et al.,1989) and, at the same time, has the advantage of a large pool of potential "predictors" but is required to invert only relatively small matrices. Since the typical matrix inversion in a OI scheme that uses stepwise

regression would typically involve three to six variables, it would appear that stepwise regression might be less costly, computationally, than operational OI systems, as will be shown.

First, two typical examples are discussed where 26 randomly distributed artificial "observations" are available. The correlations between the preliminary field departures required to determine the weights assigned to the observations [$r(\Delta_i, \Delta_j)$, $r(\Delta_j, \Delta_g)$] were specified by a very simple exponential function of the separation distances between observations (i,j) and between the analysis gridpoint and the observations (g,j).

In Case 1, the correlation $r(\Delta_j, \Delta_g)$ varied from a low of 0.11 to a high of 0.54. The intercorrelations among the observation points $r(\Delta_i, \Delta_j)$ varied from 0.02 to 0.86. In this study, as well as in the others, it was assumed that all variables were normalized with a variance of unity. Table 2 shows the weights assigned to the preliminary (first guess) field departures from the observations when all 26 observations are used in the analysis as well as the weights when only the best five observations are used. "Best" here is to be interpreted in terms of linear, least square stepwise regression.

It is apparent that there is little difference between the best five W_i whether all 26 or only these 5 observations enter the regression. Furthermore, in terms of multiple correlation ($r_{g,1,2,\ldots k}$), where k goes either to 5 (for the best five observations) or to 26 (for all observations), the results are also virtually identical; with k=5, the multiple correlation (0.6633) is numerically slightly greater than with k=26 (0.6611)*. In spite of the fact that the weight of the sixth observation of the 26 appears significant (0.0474), the remaining W_i ($i \geq 7$), which are small and largely negative, appear merely to be introducing noise. In this case at least, it would be preferable to stop the selection after 5 or 6 observations, rather than continuing to 26.

In Case 2, while the details differ, the results are similar to those of Case I. The correlations $r(\Delta_j, \Delta_g)$ varied from 0.09 to 0.50, while $r(\Delta_i, \Delta_j)$ varied from 0.01 to 0.95. Table 3 also shows the similarity in the first five selected observations, as well as the small magnitude of the weights beyond

* This is possible here, only because of round-off. All of the bivariate correlations were rounded to two decimals.

Table 2. Weights (W_i) given to the observations in Case 1, when all 26 observations are used, compared with the weights when only the best five observations are used. The multiple correlation $r_{g\,1,2,\ldots,k}$ is also shown.

i Observation Number	Weights (W_i) All Observations Used	 Best Five Used
1	0.3278	0.3320
2	0.2244	0.2267
3	0.1656	0.1737
4	0.1488	0.1475
5	0.1150	0.1001
6	0.0474	
7	0.0139	
8	0.0055	
9	0.0038	
10	0.0036	
11	0.0036	
12	-0.0012	
13	-0.0015	
14	-0.0016	
15	-0.0027	
16	-0.0038	
17	-0.0062	
18	-0.0065	
19	-0.0077	
20	-0.0079	
21	-0.0082	
22	-0.0088	
23	-0.0092	
24	-0.0093	
25	-0.0160	
26	-0.0258	
$r_{g\,1,2,\ldots,k}$	0.6611	0.6633

the sixth observation. Again, in terms of multiple correlation, virtually all of the information is contained in the best five observations. Specifically, $r_{g1,2,...,k}$ = 0.6545 with k=5 and 0.6551 with k=26.

These two cases imply that if there were a simple, rational procedure for selecting (in these cases) the best five observations, it would not be necessary to invert a matrix of 26x26, but only a 5x5. Clearly, the resulting analysis would be much more computationally efficient. Stepwise regression offers such a rational procedure.

Another experiment illustrates the application of real, densely distributed surface data. In these cases, actual analyses are made of the sea level pressure, using an OI procedure based upon multiple regression with all available observations, and then a comparison analysis, using only a small sample of these observations. In both cases the analyses based on all observations are very close to the observed value at the "gridpoint" (strictly speaking, a pseudo gridpoint).

3.3 FORWARD STEPWISE REGRESSION

To determine if a stepwise regression scheme might be useful, a reanalysis (that is, a succeeding analysis that makes use of the weights calculated in the original analysis) was performed using the OI scheme but with carefully selected observations. In OI the observations that receive very small or even negative weights apparently contribute little information to an analysis. Therefore, any observations that had been weighted with values less than 0.01 were dropped from the reanalysis. The resulting reanalysis on average used only six observations (compared to 20 observations used in the original analysis) with three of these often providing most of the information (that is, these three observations had more than 95 percent of the total weight). The reanalysis used more than nine observations at only 0.5 percent of the pseudo gridpoints. In those cases where more than six observations were retained, the weights of the additional observations were on the order of 0.01. So, given a physically reasonable structure function, OI can produce an excellent analysis with only a few carefully selected observations.

In each of the experiments the multiple correlation between the gridpoint and the retained observations did not change significantly (more than 0.003), whether 20 observations were part of the OI scheme or only the selected observations were included. In those cases where the multiple

Table 3. **Weights (W_i) in Case 2, when all 26 observations are used, compared with the weights when only the best five observations are used. The multiple correlation $r_{g1,2,\ldots,k}$ is also shown.**

i	Weights (W_i)	
Observation Number	All Observations Used	Best Five Used
1	0.2871	0.3140
2	0.2449	0.2412
3	0.2084	0.1993
4	0.1229	0.1087
5	0.1135	0.1286
6	0.0445	
7	0.0202	
8	0.0020	
9	0.0008	
10	0.0004	
11	-0.0006	
12	-0.0014	
13	-0.0018	
14	-0.0021	
15	-0.0025	
16	-0.0032	
17	-0.0050	
18	-0.0054	
19	-0.0055	
20	-0.0082	
21	-0.0083	
22	-0.0096	
23	-0.0101	
24	-0.0118	
25	-0.0124	
26	-0.0133	
$r_{g1,2,\ldots,k}$	0.6551	0.6545

correlation was slightly lower, because fewer observations entered the OI analysis, the resulting reanalysis at a gridpoint was better more often than not.

Specifically, in one experiment with 214 real observations, each of which served as a pseudo gridpoint, for 41 points the multiple correlation decreased more than 0.001 but less than 0.003 when the OI scheme used only the selected (six on average) observations. In those 41 events, the analyzed value was more accurate 26 times and less accurate 15 times. The root-mean-square (rms) difference between the observed values at all 214 points and the analyzed value at those points was 1.0062, which is slightly greater than the rms difference of 0.9648 resulting from the reanalysis. But the reanalysis reduced the bias of the average differences by a factor of 3.

It is apparent not only from the examples illustrated here but also from a large body of both theory and experience that the information contained in a large number of inter-related "predictor" variables can be closely approximated by a relatively small number of these variables or, what amounts to essentially the same thing, a small number of transformed or factorized variables. Stepwise regression is a simple procedure that produces results close to that of orthogonal transformation, but with far less computational effort. Because of the favorable results and the ease and simplicity of computation, stepwise regression is ideally suited for selecting the relevant and significant observations from the larger body of available observations, and at the same time evaluating the weights W_r. (Keegan and Shapiro, [1985] show that the selection scheme rigorously accounts for the intercorrelations among observations, and that it is a conceptual error to select observational data solely on the basis of the correlations between the observation and the analysand.)

While a variety of forms of stepwise regression are in use, a simple forward searching procedure seems appropriate for this application. Although existing computer programs may differ in detail, a simple forward stepwise regression (FSR) proceeds essentially as outlined below.

Let N represent the number of potential observations available to specify an analyzed value of the parameter at gridpoint g. A specified function has been assumed that determines (for example, as a function of the distance of separation) the intercorrelations among the N variables as well as between the gridpoint parameter and each of the N variables.

In the first step, the observation having the largest correlation with the gridpoint parameter (G) is selected. In general this will be the closest observation and is designated observation A.

In the second step (N-1), multiple correlation coefficients are obtained with G as the dependent variable and with A and, in turn, with each of the remaining (N-1) observations as independent variables. Each of these multiple correlations involves A and a different observation as the independent variables. The pair of observations yielding the largest multiple correlation is then selected. The second variable of this pair is designated as B.

In the third step (N-2), multiple correlations are obtained between G and three independent variables A, B, and each of the remaining (N-2) observations in turn. The triplet of observations yielding the largest multiple correlation is selected.

The FSR process continues in this manner until some threshold is reached. This threshold is generally specified in terms of explained variance (the square of the multiple correlation coefficient). Say that k observations have been selected by the process outlined above. The selection process stops when the square of the multiple correlation with k independent variables does not exceed that with (k-1) variables by a specified amount ε, where ε is typically 0.01 or less. That is, (k-1) observations are used when $r^2(k) - r^2(k-1) < \varepsilon$

3.4 ERROR CORRELATION STRUCTURE FUNCTIONS

From the preceding subsections, it is clear that the analysis technique relies heavily on the capability to develop physically realistic error correlation functions. These functions determine those observations that will influence an analysis at a point and how strong that influence will be.

The horizontal correlation coefficients will be fitted to the following structure functions (Mitchell et al., 1990) where sea level pressure = P, temperature = T, dewpoint = T_d, humidity = Q, u-component and v-component of wind = U and V, respectively, and height of mandatory level = UTC. For horizontal correlations of meteorological elements Z, T, Q (or T_d), and P (or Z), the raw correlations, $r(\Delta_i,\Delta_j)$ will be fitted to the function

$$HCOR_{ij} = R_b(1+\alpha)^{-1}\{ [1 + c_b d_{ij} + c_b^2(d_{ij})^2/3]\exp(-c_b d_{ij}) + \alpha[1 + c_b^2 d_{ij}/N + c_b(d_{ij})^2/3N^2]\exp(-c_b d_{ij}/N) \}$$

where $\alpha = 0.2$, d_{ij} is the distance between two observation points i and j, and N = 3. The constants R_b and c_b, both of which are different for each element, will be calculated from RWFM forecast

error statistics, as discussed in Section 4.5, and fitted with the IMSL (PL VAX Library) routine RNLIN. For winds the data will be fitted (using the IMSL routine RNLIN) to

$$HCOR_{ij} = R_v(1+\alpha/N^2)^{-1}\{ [1 + c_v d_{ij}] \exp(-c_v d_{ij}) + \alpha/N^2[1 + c_v d_{ij}/N] \exp(-c_v d_{ij}/N) \}$$

where $\alpha = 0.2$ and $N = 3$, and the constants R_v and c_v will also be calculated from RWFM forecast error statistics, as discussed in Subsection 4.5.1.

For the vertical dimension and time, the U.S. Air Force Global Weather Central Tech Note (1986) uses the following notations. The vertical correlation is represented by

$$VCOR = \{ [1 + C_1 \, LN \, [P(1)/P(2)]]^2 \}^{-1}$$

where C_1 is a positive constant determined from data discussed in Subsection 4.5.2, P(1) is the pressure at point #1, and P(2) is the pressure at point #2. If this simple function is sufficient to fit the data, it will be used; otherwise, a more sophisticated approach will be followed. The time correlation function will probably be of the form

$$TMCOR = e^{-(C\Delta T)}$$

where C is a positive constant, determined from RWFM forecast error statistics discussed in Subsection 4.5.3, and ΔT is the absolute time difference either between two observations or between observations and analysis time. The total correlation TCOR is assumed to be the product of the space and time correlations, that is,

$$TCOR = VCOR * HCOR_{ij} * TMCOR$$

The total correlation (TCOR) then replaces r_{ij} in the horizontal system of linear equations used to calculate the weights W_r.

These analytic functions will model the intercorrelations and cross-correlations of errors at observation points and the correlation and cross-correlations between an observed variable and the

first guess forecast at a gridpoint. The correlations will determine by a stepwise regression the observations that will be interpolated to a gridpoint in the OI scheme.

3.5 BUDDY CHECK

RAP project members quickly recognized the importance of developing an error checking procedure as an integral part of the observational data selection. To create such a procedure, they developed a gross error check scheme for eliminating obviously erroneous data and a buddy check for a more refined analysis. The latter scheme compares each observation with the value obtained by interpolating to the observation point without using the datum itself. Both schemes are univariate and two dimensional operating on mandatory levels one at a time.

For every point i, the buddy check scheme first selects nearby observation points and computes an analyzed value at that point by using the stepwise regression and optimum interpolation as described in Section 3.2. Then the scheme calculates analysis error, defined by the expression $d_i = A_i - O_i$, where d_i, A_i and O_i are the analysis error, analysis and the observed value, respectively, at point i.

After the calculation of d_i, A_i, and O_i for all observations points, the scheme determines the average analysis error, $\overline{d_1}$, and the standard deviation, σ_1. Any observed value with an absolute analysis error, defined as $e_i = |d_i - \overline{d_i}|$, exceeding 2.5 standard deviations becomes a candidate for rejection, and the scheme flags this value.

The scheme scrutinizes each flagged value A_i by determining its effect on every analysis value, A_j affected by A_i (i.e., those points where the analysis uses O_i as one of the observations to interpolate). To recheck each A_i, the scheme first reanalyzes every A_j by excluding the flagged value O_i. Next the scheme calculates the $\overline{d_2}$ as the mean analysis error for the subfield that excludes all flagged points and the weighted difference D_i, defined by the expression

$$D_i = W_i \sum_{j=1}^{n_i} |A_j - O_j - \overline{d_1}| - \sum_{j=1}^{n_i} |A_j' - O_j - \overline{d_2}|$$

where $W_i = e_i / (2.5*\sigma_1 + \overline{d_1})$, n_i is the number of points used to calculate A_i, A_j' is A_j recalculated

by excluding O_i, and O_j is the observed value at point j. The factor W_i exceeds unity for all flagged values and magnifies the effect of the absolute analysis errors.

If D_i is positive, then removal of O_i reduces the average analysis error at all points j, and O_i sufficiently degrades the analyses at those points to warrant rejection. Otherwise, if D_i is negative, excluding O_i will make the analyses at the neighboring points worse and, therefore, the scheme removes the flag and preserves the observed value.

4. DATABASE SPECIFICATION

Much of the effort expended on RAP has been on the development of extensive databases. These include databases of analyses, forecasts, observations, forecast error correlations, and data required for observing system simulation experiments. Each of these databases is described.

4.1 ANALYSIS DATABASE

All HIRAS data needed to initialize the GSM or to verify the RWFM or RAP was saved on magnetic tapes. There are 62 files per month for July 1988 and January 1989. Each file has 15 mandatory levels and 10,585 (145x73) gridpoints per level. The 15 levels are at 1,000 mb, 850 mb, 700 mb, 500 mb, 400 mb, 300 mb, 250 mb, 200 mb, 150 mb, 100 mb, 70 mb, 50 mb, 30 mb, 20 mb, and 10 mb. No surface data except sea level pressure is included because RAP can be verified better there with actual observations or other techniques. The lower six levels contain U, V, T, Q (both specific and relative humidity), and D-values (that is, the difference between the measured height and standard height at the given level); levels 7 through 15 contain similar data except no humidity is available. The HIRAS data needed for verification were interpolated onto the RWFM grid in the windows in the Eurasian (EU) and Central American (CA) windows.

4.2 FORECAST DATABASE

The GSM was initialized from HIRAS on both 1 January 1989 at 00 UTC and 1 July 1988 at 00 UTC and at 2.5 day intervals thereafter during those months, yielding 12 independent 36 hr forecast cycles for January and July. The spectral coefficients of the nonlinear mode initialization

(NMI) and the 6-hr forecasts of surface pressure. wind components, temperature, and humidity were postprocessed to a 2.5° grid on mandatory levels, and saved. Then two 36 hr GSM and RWFM forecasts were executed (the RWFM boundary conditions came from the GSM forecasts), one in the Eurasian (EU) and the other in the Central American (CA) regions. Both the GSM and RWFM forecasts were subjectively and objectively compared to each other and to HIRAS (see Appendix B.) to ensure that only acceptable forecasts were in the database.

These RWFM forecasts will be interpolated to the RAP window on the uniform gridded data field (UGDF) grid, which will be used as the RAP grid. To be consistent with AFGWC, STC implemented the RWFM in the operational mode of 16 σ-level 61x61 grid with a horizontal resolution of 95 km. The UGDF grid system has a horizontal resolution of 50 nm at mandatory levels up to 50 mb; the EU window is on a polar stereographic projection, and the CA window is on a Mercator projection.

The RAP window has 40x40 UGDF grid boxes, but the RWFM has 60x60 grid boxes (each of which is slightly larger than a UGDF box). Thus, the RAP window can fit inside the RWFM window such that first guess forecasts are available several hundred miles beyond the RAP boundaries. (These forecasts are needed to calculate errors of observations outside the RAP window that affect gridpoints near a boundary.)

The following RWFM forecasts at 12, 18, 24, and 36 hr are stored as RAP first guess fields for both regions and seasons: on the surface, sea level pressure and temperature; at all mandatory levels of temperature, height, and u and v components of wind; and at the lower six mandatory levels of relative and specific humidity.

4.3 OBSERVATION DATABASE

The development of the observation database required decoding, sorting, and merging of data extracted from 34 magnetic tapes from the USAF Environmental Technical Applications Center. All observations were ordered by station number with data in daily sequence for the entire month. The database required synoptic observations.

Observations closest to (-3 to +1 hr) 00 UTC, 06 UTC, 12 UTC, and 18 UTC have been stored for use in the CA and EU windows. The observation window is approximately the size of RWFM (60x60 grid boxes, each box 95x95 km). The observations were extracted by station for sorting and merging into the windows by season and time.

The data are surface observations of sea level pressure (P), temperature (T), dewpoint (T_d), and station elevation; upper air (RAOB) observations of u and v components of wind (U and V, respectively,), height of mandatory level (Z), T, and T_d ; aircraft observations of U, V, T, latitude/longitude, assigned pressure level, and time; and unique satellite observations of T and Z in the form of a RAOB.

4.4 OBSERVATION SYSTEM SIMULATION EXPERIMENT DATABASES

The OSSE databases form the beginning of a complex data processing project. The simplest and possibly most meaningful description of the databases is shown in Fig. 1.

4.5 ERROR CORRELATIONS DATABASE

From Section 3.4 there are three separate error correlations required: horizontal, vertical, and temporal. The correlations are calculated from the differences at observation points between forecast and observed values. These differences (the Δ_is from Eq. 2) are calculated on each of the mandatory levels after horizontal interpolation of forecast (first guess) values from gridpoints to observation points, using the four-point restorer scheme (Shapiro, 1978). Observations that match the times of RWFM forecasts are interpolated vertically if necessary to mandatory levels (1,000 to 50 mb) for January 1989 and July 1988 in the CA and EU windows. Observations of Z, T, T_d, U, and V not on mandatory levels are interpolated linearly in ln P to the closer mandatory level.

Let $\Delta_i = f^p_i - f^o_i$ be the forecast error at an observation point i, where from Eq. 1, f^p_i is the preliminary (first guess forecast) value of a meteorological element at observation point i, and f^o_i is the observed value at observation point i. The Δ_is can be calculated for each of the forecasts in the database of Section 4.2, given the observed elements in Section 4.3. They are defined only when forecast and observed elements are both available at nearby times and locations.

4.5.1 Horizontal Error Correlations

The Δ_is are a function of forecast length, mandatory level, month, instrument, distance between and relative orientation of observations, and window. Table 4 illustrates a general error database, which for horizontal correlations requires the Δs at specific distance intervals and direction vector intervals between observations pairs. The mean (M_i) and the standard deviation (σ_i) of each error variable is calculated and stored by summing the Δs over the 12 forecasts for each level, month, window, and forecast length for all observation points (i), ignoring any point that has less than eight observations.

$$M_i = (\Sigma_i \Delta_i)/n \text{ and } \sigma_i = \{ [1/(n-1)] * [\Sigma_i \Delta_i^2 - M_i^2 * n] \}^{1/2}$$

where n is the number of forecasts with observations that match in time and $8 \leq n \leq 12$.

The error at each observation point in the set is correlated with the error at the other observation points for all variables. Let r_{ij} be the (univariate) autocorrelation coefficient,

$$r_{ij} = (\overline{\Delta_i * \Delta_j} - \overline{\Delta_i} * \overline{\Delta_j})/(\sigma_i * \sigma_j) \tag{4}$$

for observation point i and observation point j of the same meteorological error element, where the overbar is an average over n. Note that

$$(\overline{\Delta_i * \Delta_j} = \overline{\Delta_j * \Delta_i})$$

Similarly, for different meteorological elements, say A and B, a (bivariate) cross-correlation can be written

$$r_{A_i B_j} = \frac{(\overline{\Delta_{A_i} * \Delta_{B_j}} - \overline{\Delta_{A_i}} * \overline{\Delta_{B_j}})}{(\sigma_{A_i} * \sigma_{B_j})} \tag{5}$$

observed element (identified if measured by aircraft or satellite) in the database will be calculated where Eq. 4 is the special case of a = b from the more general Eq. 5. (Both equations can be used to calculate any type of correlation between two elements.) For both windows and months on all levels at all forecast lengths, the univariate and bivariate horizontal correlation coefficients for each

Table 4. The generalized error database at observation point i for some specified level, month, meteorological element, and window

Initial Forecast	+12-hr	+18-hr	+24-hr	+36-hr
1 / 00 UTC	$\Delta_i(1,1)$	·	·	$\Delta_i(1,4)$
3 / 12 UTC	$\Delta_i(2,1)$	·	·	$\Delta_i(2,4)$
6 / 00 UTC	·	·	·	·
8 / 12 UTC	·	·	·	·
·	·	·	·	·
·	·	·	·	·
28/12 UTC	$\Delta_i(12,1)$	·	·	$\Delta_i(12,4)$

and stored for each unique pair of observations (i,j). The correlations will be stored by instrument, month, length of forecast, and mandatory level into bins, which organize paired observations by the distance between them (Thiebaux et al., 1986) in 50-km intervals out to 2,500 km. In addition to placing the correlation pairs into bins that are a function of only the distance between the pairs, the correlations are also "binned" according to the direction of the line connecting the paired points. The purpose of treating the line as a vector is to allow a determination of the isotropy of error correlation. Thus, there will be a group of horizontal correlation coefficients arranged as shown in Table 5.

This database leads to a complex horizontal error correlation model. The approach, however, is to let the data speak for themselves; therefore, no univariate or multivariate combinations of meteorological elements can be eliminated arbitrarily from consideration. Consequently, horizontal error correlations are calculated for Z-Z, T-T, U-U, V-V, Q-Q, Z-T, Z-U, Z-V, Z-Q, T-U, T-V, T-Q, U-V, U-Q, and V-Q. In addition, the multivariate correlations, say r(A,B), are calculated for both r(A,B) and r(B,A). Also, there are four instruments to consider: aircraft, rawinsondes, and two satellites. Finally, there are four quadrants to account for the direction of the vector connecting two observation points, four forecasts lengths, two windows, and two seasons.

Table 5. The horizontal correlation database for windows, seasons, and levels for each observed unique pair of observations

	Distance (km)				
	0-50	51-100	101-150	...	2451-2500
Instrument	.	.	.	.	.
Europe	.	.	.	.	.
Central America	.	.	.	.	.
12-hr forecast	.	.	.	.	.
18-hr forecast	.	.	.	.	.
24-hr forecast	.	.	.	.	.
36-hr forecast	.	.	.	.	.
January	.	.	.	.	.
July	.	.	.	.	.
Quadrant					
NE	.	.	.	.	.
NW	.	.	.	.	.
SW	.	.	.	.	.
SE	.	.	.	.	.

Thus, the horizontal error correlation model is a function of several thousand variables! Undoubtedly, the model will be simplified because many of these variables will not be unique; nevertheless, the data will be allowed to speak for themselves.

4.5.2 Vertical Error Correlations

Similarly, the univariate and bivariate vertical error correlation coefficients of all the meteorological elements (Z-Z, T-T, U-U, V-V, Q-Q, Z-T, Z-U, Z-V, Z-Q, T-U, T-V, T-Q, U-V, U-Q, and V-Q) will be calculated and averaged over all radiosonde sites in the database. Satellite data are limited to error correlations of Z-Z, T-T, and Z-T. Of course, in this case there are no bins for the distance between observation pairs or the direction vector between them. These correlations are being computed rigorously for all mandatory levels, as shown in Table 6.

Consider the vertical error correlation of element A on level k with element B on level l at a rawinsonde observation point, $r_{kl}(\Delta A_k, \Delta B_l)$ [for example, $r(\Delta A_{850}, \Delta B_{700})$, where A is on the 850-mb level and B is on the 700-mb level]. The Δ_is are calculated as shown in Table 4, and the correlations are calculated from Eq. 5. The vertical correlations are functions of several variables: the instrument; the months of January and July; the EU and CA windows; and the four forecasts: 12 hr, 18 hr, 24 hr, and 36 hr). The averages are stored in Table 6.

4.5.3 Temporal Error Correlations

Finally, the univariate and bivariate temporal error correlation coefficients of all the meteorological elements will be calculated and their averages stored for Z-Z, T-T, U-U, V-V, Q-Q, Z-T, Z-U, Z-V, Z-Q, T-U, T-V, T-Q, U-V, U-Q, and V-Q. In addition, the multivariate correlations, say r(A,B), are calculated for both r(A,B) and r(B,A). This is a comparatively simple (because there are only four forecast times) calculation of correlating the Δ_is at a given forecast time with the other forecast times.

Consider, for example, meteorological elements A and B (recall that A = B for univariate correlations), the temporal error correlation is given by the general expression $r_{m,n}(\Delta A_m, \Delta B_n)$ where m is the m^{th}-hr forecast and n is the n^{th}-hr forecast. Specifically, there are six unique temporal error correlations: $r_T(\Delta A_{12h}, \Delta B_{18h})$, $r_T(\Delta A_{12h}, \Delta B_{24h})$, $r_T(\Delta A_{12h}, \Delta B_{36h})$, $r_T(\Delta A_{18h}, \Delta B_{24h})$, $r_T(\Delta A_{18h}, \Delta B_{36h})$, and $r_T(\Delta A_{24h}, \Delta B_{36h})$. These correlations require the Δ_is from Table 4 and are calculated from Eq. 5. The temporal error correlations are functions of the same variables as are the vertical correlations. The variables are the rawinsondes, the months of January and July, the EU and CA windows, and the mandatory levels. The average correlations are stored as shown in Table 7.

5. CASE STUDIES OF NUMERICAL ANALYSIS EXPERIMENTS

The OI experiments with real data have yielded many interesting and relevant results. The numerical experiments discussed in Section 3 that used simulated data were theoretically interesting and useful; however, real data offered more robust experiments and practical results. Simulated error correlation coefficients were still required, however, because the models being developed under STC Task 2 were not ready for use.

Table 6. The average over all rawinsonde sites of the vertical error correlations of all observed meteorological elements at the given level with the levels above for each window (Eurasia and Central America), month (January and July), and forecast hour (12, 18, 24, and 36).

Standard Levels (mbs)										
1000	1000	1000	1000	1000	1000	1000	1000	1000	1000	1000
850	700	500	400	300	250	200	150	100	70	50
	850	850	850	850	850	850	850	850	850	850
	700	500	400	300	250	200	150	100	70	50
		700	700	700	700	700	700	700	700	700
		500	400	300	250	200	150	100	70	50
			500	500	500	500	500	500	500	500
			400	300	250	200	150	100	70	50
				400	400	400	400	400	400	400
				300	250	200	150	100	70	50
					300	300	300	300	300	300
					250	200	150	100	70	50
						250	250	250	250	250
						200	150	100	70	50
							200	200	200	200
							150	100	70	50
								150	150	150
								100	70	50
									100	100
									70	50
										70
										50

Table 7. The average temporal forecast error correlation database for windows, months, instruments, mandatory levels, and observed elements.

	Forecast Hour			
	12th	18th	24th	36th
Europe	.	.	.	.
Central America	.	.	.	.
January	.	.	.	.
July	.	.	.	.
Mandatory Levels	.	.	.	

The error correlation model followed Thiebaux et al. (1986), who found that the second order autoregressive function called SOAR worked well with meteorological data. Franke (1990) used their general expression

$$C(s) = (1+A)(1+as)e^{-as} + A$$

where s denotes distance, and a and A are parameters determined by fitting the data.

Our experiments used a very simple version of SOAR to compute the correlation coefficient required in Eq. 3 between observation points 1 and 2, $r_{12} = e^{-\sigma d}$, where d is the distance in kilometers between the two points, and σ is a scaling parameter arbitrarily determined such that $r_{12} = 0.01$ at the extent of the chosen radius of influence. Thus, in this simple version of SOAR no real data are fitted to determine σ. (For example, when d = 500 km, σ = 0.0092, and when d = 1000 km, σ = 0.0046.) So from $r_{12} = e^{-\sigma d}$, the simulated correlation coefficients were calculated as a function of the distance between observations and the selected point, and the intercorrelations were calculated as a function of the distance between the observations.

The results of Section 3.2 provided STC with insight into data selection techniques by showing how well an OI analysis at observation points matched verifying observations there. The results in turn suggested several follow-on experiments. A description of the most noteworthy case studies, their results, and conclusions follow.

5.1 ANALYSIS AT PSEUDO GRIDPOINTS

First, a database of the sea level pressure in two windows was prepared. The database identified the latitude and longitude of all surface observation points in AFGWC regions in the EU and CA windows at a time for which a 24-hr RWFM forecast was available.

Using the four-point restoring interpolation scheme of Shapiro (1978), the first guess field (from the 24 hr RWFM forecast) at gridpoints was interpolated to each observation point. The four-point restorer scheme, which interpolates from 16 surrounding gridpoints on a plane to an observation point, interpolates data on a grid to an observation point. The advantage of this scheme is that it, as a high order, linear interpolation scheme, corrects the phase distortion and amplitude damping of ordinary linear (two-point) interpolation. Also, the restoring interpolation operator is computationally simpler and more accurate than cubic splines for interpolation from a uniform grid.

The forecast error, Δ_i (defined here as observed pressure minus interpolated pressure), was calculated for all observation points (i). Then the iterative analysis procedure for the window selected one at a time all observation points, each of which served as a "pseudo" gridpoint for purposes of this experiment. Each point and up to 20 of the closest observations within, say, 500 km (or some other given radius of influence) of this point made up a set of observations.

Each of these initial numerical analysis experiments in optimum interpolation, taking the lead from Sections 3.1 and 3.2, had two parts, the second following from the first: (1) an original analysis at an observation point that used up to 20 of the closest observations within an arbitrary radius of influence, and (2) a follow-on analysis at each point that used a selected subset of the observations from the original analysis at the point.

The original analysis at a selected point was calculated from the interpolated first guess at that point, plus the sum of the product of the weights and the errors at up to 20 of the closest observation points (see Eq. 1). The weights were calculated by inverting the correlation matrix from Eq. 3. The procedure stopped after an analysis was performed at all observation points (which are treated as pseudo gridpoints). This analysis is called OI-1. The analyzed values were compared with the observed values at all points. The rms errors and average errors of forecasts and analyses determined the goodness of the OI analysis scheme.

The second part of this experiment is a follow-on analysis performed at each observation (pseudo gridpoint). This second analysis used *only* observations from the original analysis at points with weights $W_i \geq 0.01$ (see Tables 2 and 3) to influence the point to which observations were being interpolated. In other words, for the second analysis, which is called OI-2, Eq. 1 was solved for a restricted subset of the N observations. The effect was to use the set of observations that maximized the information provided to the analysis from a limited number of observations.

This experiment was clearly not designed as a candidate for an operational numerical analysis scheme. The purpose was to show that a greatly reduced subset of observations available to perform an analysis at a point is sufficient to provide an analysis nearly equivalent to one produced by using all available observations within some chosen radius of influence. Some of the most pertinent results of these experiments follow. Given several good observations that are evenly distributed, the OI scheme produced an excellent analysis (even with a poor first guess and a simple structure function).

In Europe, where most surface observations are close together, the two or three observations with the highest correlations (between the gridpoint and observations as well as intercorrelations between the observations) are heavily weighted, so OI in effect ignored observations with small weights, as required by Eq. 1. The experiment first used the 20 closest observations within 500 km of a selected point for the OI analysis, and invariably three or less observations carried nearly all the weight. Even on the boundary or at remote points, where as few as eight observations were within 500 km, less that half of those observations had much effect on the analysis.

Other experiments also yielded results that confirmed intuitive expectations but needed documentation nonetheless. For example, an obviously erroneous observation, which had a surface pressure of 911 mb in a pressure field that averaged 1,010 mb, got into the database (due to incomplete error checking at that time). Whenever that observation was close to a selected point and therefore was given a high correlation, the analyzed value from OI was bad, no matter how good the first guess was. This example pointed out the critical requirement for using a gross error check, and it suggested the need for using a buddy check.

Experiments in the CA window, a data-sparse region compared to Eurasia, illustrated how OI performed with less data. The first guess forecast in July is excellent; consequently, the OI analysis scheme is challenged to make a noticeable improvement from the preliminary field. The average difference between the first guess field interpolated to the 211 observation points and the observed values was only 0.59 mb. Experiments with three different radii of influence were conducted: the standard radius of influence of 500 km, one shortened to 250 km, and one extending to 750 km. The purpose was to check how additional observations would improve the analysis.

1. *250-km radius of influence from gridpoint to the observation*

   Only four observations on average entered the analysis at a gridpoint for this case. The average difference between the analysis and the observed values was 0.415 mb. The second analysis, which typically used 60 percent of the observations in the original analysis, had an average difference of 0.417 mb.

2. *Radius of influence extending out to 500 km*

At this radius of influence, however, a mean of 12 observations were included in the OI. The average difference between the original analysis and the observed values was 0.242 mb. The second analysis, which selected only one-third of the observations from the original analysis, had an average difference of 0.236 mb. The rms differences were essentially the same too.

3. *Radius of influence extending out to 750 km*

The OI scheme used 15 observations on average. This approach improved the analysis slightly (but not significantly) by reducing the bias; however, the rms differences were virtually the same as Case 2. Given an error correlation model that decreases exponentially with increasing distance, it was predictable that extending the radius of influence beyond some optimum distance would result in little improvement of an analysis. These expectations are now confirmed in practice.

5.2 SELECTING OBSERVATIONS BY FORWARD STEPWISE REGRESSION

From the above case studies and Section 3, it can be concluded that a second analysis, even though using a subset of observations, was nearly as "good" (approximately the same) as the original analysis, obtained from interpolating the full set of N observations (Eq. 1). Too many observations, most with weights so small they apparently introduced noise rather than information, did little to improve an analysis. On the other hand, carefully selected observations allowed OI to perform more efficiently but as effectively. The selection technique of Section 5.1, however, obviously would be too cumbersome in practice to be of value even though it worked in theory. Clearly, it makes no sense to run a complete analysis, which requires the inversion of the large matrix in Eq. 2, for the sole purpose of identifying a subset of the "best" observations to influence an analysis point. Sections 3.2 and 3.3 determined a better method, forward stepwise regression. Consider the following case studies.

5.2.1 Sea Level Pressure Analyses

The first test of the FSR scheme was to select sea level pressure observations. Recall from Section 3.2 that the efficiency of the FSR scheme is regulated by ε. With ε = 0.001, 0.005, and 0.01 in three different experiments performed in both data-sparse and data-rich regions, the smaller values of ε served to force more observations into affecting the analysis. When $\varepsilon < 0.01$ the additional observations had very small weights, and the analysis hardly improved. On average, including the additional observations resulted in an error reduction of less than 0.04 mb; the maximum reduction was less than 0.1 mb.

Table 8 shows a typical example of the effectiveness of the FSR technique. The frequency distribution of the number of observations required for an analysis is highly skewed towards fewer observations. The western Eurasian region contained 208 observations used as pseudo gridpoints, about each of which an OI analysis was performed using observations selected by the FSR. The results from the FSR are compared to two prior analyses made at the same points: the original analysis (OI-1) made from the complete set of those 20 observations and the second analysis (OI-2) made from the subset of observations with weights $W_i \geq 0.01$. Each of the 208 observation points had at least 20 observations within 500 km.

The FSR technique is obviously computationally superior to the OI-2 technique because OI-2 first required an inversion of a 20x20 matrix followed by a second inversion of a matrix of a size shown in Table 8, on average a 6x6 matrix. On the other hand, the FSR requires the inversion of many small matrices, whose maximum size is shown in the table but typically is only a 3x3 matrix.

Similarly, selecting observations by the FSR for an OI analysis is better than using the 20 observations in the OI-1 analysis. On average the FSR needed to select only three observations for an excellent OI analysis. Table 9 shows two representative measures of error in an analysis of the surface pressure over western Eurasia, where the OI original analysis made use of the 20 closest observations (OI-1), which were not rigorously selected. For this case the average first-guess error (forecast minus observed pressure) is -7.49 mb, and the rms difference between the forecast and observation is 8.23 mb.

Table 8. Frequency distribution of the occurrence of the given number of observations used in an OI analysis at observation points in a data-rich region. The OI-2 is the second analysis at a point that resulted when only observations with $W_i \geq 0.01$ were selected from a set of the 20 closest observations, which influenced the original analysis OI-1 at the point. The FSR is the analysis that resulted from optimum interpolation of observations selected by the forward stepwise regression.

	Number of observations									
	2	3	4	5	6	7	8	9	10	11+
OI-2	3	12	16	36	47	38	32	20	8	2
FSR	81	79	47	6	1					

Table 9. Comparison of analysis errors in millibars. The OI-1 is the case where the observations are not rigorously selected, that is, up to 20 observation within 500 km are used. The OI-2 and FSR are described in Table 8.

	OI-1	OI-2	FSR
Average of Observed Minus Analyzed Pressure	-0.34	-0.12	-0.34
RMS Difference Between the Observation and the Analysis	1.00	0.96	1.00

Clearly, the OI results in an excellent analysis, with an average error reduction of 94 percent and an rms error reduction of 88 percent. But the FSR is remarkable because it needs so few observations to make the OI effective. The point is that these observations are objectively selected by stepwise regression. Note that the reduction of average error and rms error is only slightly smaller for the OI-2 case. Also, the FSR selects on average three observations whose OI yields an analysis virtually the same as one produced from the full set of 20 observations.

Similar results for surface pressure analyses occur over a data-sparse region, in this case a region extending from northern South America to the southern United States. Table 10 shows that

the number of observations affecting an analysis (that is, the number of observations within 500 km of each of 201 observation points) for this region has several peaks spread across the spectrum.

Only 25 percent of the points have a complete set of 20 observations within 500 km. (Earlier experiments showed that extending the radius of influence from 500 km to 750 km had little effect on the analysis.) Note that only slightly more than two observations on average are selected by the FSR for an OI analysis compared to (a) an average of nearly 12 observations in the OI-1 group, and (b) the slightly more than four observations (with $Wi \geq 0.01$) selected from the OI-1 group for use in the OI-2 analysis.

But, as shown in Table 11, the results are similar, even in a data-sparse region when the first guess itself was a good analysis. For this case the average first guess error (forecast minus observed pressure) is only 0.59 mb, and the rms difference between the forecast and observation is only 2.42 mb.

Clearly, the FSR is an outstanding technique for use in practice because it is both so computationally efficient and accurate. In this case, however, the first guess was very good; so OI could reduce the average error only by 60 percent and the rms error by only 18 percent. Nevertheless, the FSR scheme accomplished the reduction by using only a few observations, rather than attempting to squeeze information, which does not exist in a least squares sense, from a host of superfluous observations.

Table 10. Frequency distribution of the number of observations used in the optimum interpolation analysis to interpolate a value to a point in a data-sparse region. The OI-1, OI-2, and FSR have the same meaning as in Table 9.

	Number of observations								
	0	1	2	3	4	5	6-10	11-15	16-20
OI-1	4	4	5	8	14	5	51	47	73
OI-2	4	8	22	38	51	41	26	0	0
FSR	4	24	128	45	10	0	0	0	0

Table 11. Comparison of analysis errors (in millibars) at observations points used in an OI analysis in a data-sparse region. The OI-1, OI-2, and FSR are the same as in Tables 8 and 9.

	OI-1	OI-2	FSR
Average of Observed Minus Analyzed Pressure	0.24	0.24	0.28
RMS Difference Between the Observation and the Analysis	2.10	2.10	2.15

5.2.2 500 mb Height Analyses

With 500-mb heights replacing surface pressure, similar experiments would be generally expected to yield similar results. Since the upper air data is sparse compared to surface data, however, the radius of influence of the correlation function was extended to 1,000 km to allow more potential observations to influence the analysis.

This case is a study of 180 observations over Eurasia on 9 January 1989 at 1200 UTC. The FSR scheme was as effective at 500 mb as it was at the surface. On average the FSR used only 17 percent of the available observations surrounding each pseudo gridpoint; nevertheless, it produced an analysis similar to one obtained by using all the observations within 1,000 km. Specifically, the rms error of the FSR analysis was 76 percent of the error in the first guess; the rms error of the OI-1 analysis (all observations within 1,000 km are used) was 74 percent of the error in the first guess.

Table 12 shows the wide range of the number of observations in the OI-1 group and the effect of the FSR on how many of those observations are needed for an analysis. It is impressive that on average about three observations around a gridpoint can make an analysis nearly as good as about 17 observations.

As shown in Table 13, the results are excellent, even though the average first guess error (forecast - observed) is only -12.4 m and the rms difference is 28.7 m. The FSR improves the analysis considerably. The average error is reduced by almost two-thirds and the rms error is reduced by about one-quarter.

Table 12. Frequency distribution of the number of observations at 500 mb used in an OI analysis of heights to interpolate a value to a point. The OI-1 and FSR are the same as in Tables 8 and 9.

	Number of observations								
	0	1	2	3	4	5	6-10	11-15	16-20
OI-1	0	0	0	0	4	2	18	30	126
FSR	0	5	65	79	29	2	0	0	0

Table 13. Comparison of 500-mb height analysis errors in meters. The OI-1 and FSR are the same as in Tables 8 and 9.

	OI-1	FSR
Average of Observed Minus Analyzed Height	-3.2	-4.3
RMS Difference Between the Observation and the Analysis	21.2	21.9

A close study of the detailed output of the experiments revealed some interesting results. At slightly more than 20 percent of the points the FSR yielded a better analysis than OI-1, even though the FSR used much fewer observations. At almost 6 percent of points the first guess was better than the analyses, but the errors were very small. The maximum difference between the errors resulting from FSR and OI-1 was less than 10 m. Taking all the results together, the FSR reduced the average rms error by 30 percent, and OI-1 reduced the average rms error by 32 percent. Both schemes reduced the average error by 40 percent.

In sum, optimum interpolation performed an excellent analysis, as anticipated. Forward stepwise regression made the general OI scheme even more efficient.

5.3 ANALYSES ON THE RAP GRID

Next, analyses were performed at actual gridpoints rather than the pseudo grid (that is, observation) points, as in the preceding experiments. Each gridpoint and up to 20 of the closest observations within 500 km (or some other given radius) of this point made up a set of observations. (Recall that this analysis is called OI-1.) From this set the simulated correlation coefficients were calculated (from the model $r_{ij} = e^{-\alpha d}$) as a function of the distance between observations and the gridpoint, and the intercorrelations between each of the observation points were calculated as a function of the distance between the observations.

Several numerical experiments provided both objective and subjective results that demonstrated the success of the transformation of the OI scheme. The baseline test is a comparison of two analyses, one at observation points and the other at gridpoints, using the same first guess and observation set. In all cases both analyses were similar. The second test compares an analysis calculated from the OI using a set of up to 20 of the closest observations (OI-1) with an analysis calculated from a subset of those observations chosen by the FSR process. This test confirmed the technical approach of integrating stepwise regression into optimal interpolation. All meteorological variables were analyzed.

The objective "measure of merit" is a comparison of the errors (the difference between the value of an element at an observation point and the value obtained by interpolating the element at surrounding gridpoints to the observation point). This "grid-to-station" verification is not a perfect measure of merit; nevertheless, it is useful.

5.3.1 Sea Level Pressure Analyses

First, however, note from Table 14 that only a relatively few observation of sea level pressure are needed to produce an accurate analysis in a data-rich region. Of course, the FSR technique is computationally superior to the OI-1 technique, which required an inversion of a large (on average an 18x18 in this case) matrix. On the other hand, the FSR required the inversion of many small matrices, usually a 3x3 matrix, as shown in Table 8. On the 41x41 RAP grid (1,681 gridpoints), the reduced number of calculations needed for the FSR scheme is obviously substantial.

Table 14. Frequency distribution of the number of sea level pressure observations used in an OI analysis to interpolate a value to a point in a data-rich region on the RAP grid system. The OI-1 and FSR are described in Tables 8 and 9.

	Number of observations							
	1	2	3	4	5	6-10	11-15	16-20
OI-1	0	0	0	0	0	31	329	1,321
FSR	240	660	622	148	11	0	0	0

The analyses were accurate, as measured by the reduction of average and root mean differences; however, plots of the sea level pressure appeared to be "noisy." Note from Eq. 1 that an OI analysis results from adding the first guess field to the sum of the weighted departures ($\Sigma_i W_i{*}D_i$). These corrections are slightly noisy when viewed as analyzed plots of the departure fields at gridpoints. Also, lagged autocorrelations and Fourier analyses of the fields suggest there is some two-grid-interval variations (noise). These small-scale variations were removed, without harming the overall analysis, by applying Shapiro's seven point linear smoothing filter (Shapiro, 1975). It suppresses two-grid-interval waves without changing the phase of any wave component and with little damping of the amplitudes of all other waves.

5.3.2 500-mb Height Analyses

Statistics of analyses of 500-mb height surfaces performed at pseudo gridpoints are similar to those performed on a grid. On average the OI with the FSR selecting the observations required only three observations to make an analysis nearly identical to an OI analysis that used an average of 18 observations surrounding each gridpoint. Overlaid plots of the two 500-mb analyses revealed only the slightest of differences between the two, and those differences were isolated. Table 15 shows two measures of merit in an analysis of the 500-mb height field over western Eurasia. For this case with a good, unbiased first guess the average error (forecast minus observed) is only 10 m, and the rms difference between the forecast and observation is approximately 24 m. The average rms difference between the OI-1 and FSR (not shown) is 2.8 m, or 12 percent of the first guess error.

For comparison Table 16 shows the results of analyses that use the same first guess and observation set but are calculated at observation points instead of gridpoints. In this case the

Table 15. The 500-mb differences (FIRST GUESS analysis) in meters, using the OI on a 50-nm grid over data-rich Eurasia. The OI-1 and FSR are described in Tables 8 and 9.

	OI-1	FSR
Average Value	9.97	9.25
Root-Mean-Square	24.2	23.0

Table 16. The 500-mb analysis errors (m) using the OI at the observation points over the Eurasian region. FIRST GUESS is the RWFM (preliminary) forecast field interpolated to the observation points.

	FIRST GUESS	OI-1	FSR
Average of Observed Minus Analyzed	-15.9	-1.18	-2.15
RMS Difference Between the Observation and the Analysis	34.7	6.2	6.9

average first guess error was nearly -16 m as compared to analysis errors of only about 2 m. The first guess rms errors (that is, the difference between the first guess and the observed 500-mb height) was about 35 m compared to analyzed rms errors less than 7 m.

Clearly, the OI results in an excellent analysis, with an average error reduction of 86 percent for the FSR and 92 percent for the OI-1, and an rms error reduction of about 80 percent for both. Again, the FSR needs so few observations to make the OI effective because these observations are objectively selected by stepwise regression. Note that the FSR reduction of average error and rms error is only slightly larger than the OI-1 case, even though the FSR selects on average only three observations from the full set of up to 20.

5.3.3 The 500-mb Temperature Analyses

Similar results for 500-mb temperature analyses occur over a data-sparse region, in this case the region extending from northern South America to the southern United States. (As shown, however, the distribution of observations is not like that of Table 13.) In fact, a composite summary of several analyses of different variables in the two regions yields the same conclusions as the

individual case illustrated in Tables 9, 10, and 11. The rms errors of the analysis are typically only 20 percent of the rms errors of the first guess. The FSR and OI-1 analyses are remarkably similar as well as a great improvement over the first guess. The autocorrelation of both analyses is typically 0.99 for a data-rich region and 0.97 for a data-sparse region. Of course, the amount of improvement depends upon the quality of the first guess forecast.

5.3.4 The 500-mb Humidity Analyses

The excellent performance of the stepwise regression scheme in the optimum interpolation of pressure, both on the surface and on isobaric levels, and temperature leads to the conclusion that using a set of carefully selected observations is preferable to using all observations in some arbitrary vicinity. The next test of the OI scheme was to analyze the more difficult meteorological variables, of humidity and wind.

In spite of poor first guess forecasts of moisture, the OI scheme produced good analyses of humidity (using the method of Redder and Fukuta (1989) to convert from dewpoint to standard humidity variables), even though the scheme has a simple univariate correlation function. The rms errors and average errors were similar to those of other variables.

The objective test continues to compare an analysis calculated from the OI using a set of up to 20 of the closest observations (OI-1) with an analysis calculated from a subset of those observations chosen by the FSR process. In addition, both these analyses can be made at either gridpoints or observation points, which serve as pseudo gridpoints; hence it is straightforward to compare analyses to actual observations too. This test confirmed the technical approach used to integrate stepwise regression into optimal interpolation, and with a simple but physically realistic correlation function. The objective measure of merit is a comparison of the errors (the value of an element at an observation point minus the value obtained by interpolating the element at surrounding gridpoints to the observation point).

Table 17 shows the average errors and rms errors of the 500 mb relative humidity analysis and confirms the similarity between analyses using an average of 17 observations (OI-1) and the analysis derived from optimum interpolation of observations selected by FSR. These two analyses

Table 17. The difference between the FIRST GUESS (a 36 hr RWFM forecast) and the relative humidity analysis on a grid over Eurasia. The OI-1 is an analysis computed from a complete set of observations, and the FSR is the analysis computed using forward stepwise regression, which selects a subset of observations.

	OI-1	FSR
Average Value (%)	0.125	0.052
Root-Mean-Square (%)	15.9	15.67

over western Eurasia are clearly similar, but they need to be complemented by a measure of merit that compares errors at observation points.

Analyzing the errors at the observation points themselves, rather than at the gridpoints as in Table 17, gives a better measure of accuracy of the scheme. Table 18 shows that the scheme is successful; the rms errors are reduced by 83 percent. In addition, the correlation between the analyzed humidity field interpolated to the observation points and the humidity measured at the observation points is 0.97 (the corresponding first guess correlation is 0.41).

Thus, even with a poor first guess, the OI scheme produces an excellent humidity analysis. Note that the FSR reduction of average error and rms error is only slightly smaller than the OI-1 case, even though the FSR selects on average only three observations from the full set of up to 20 observations nearest the gridpoint.

Table 19 shows the various correlations among the analyzed humidity fields with each other and with actual observations. The analyzed field is very highly correlated with the observed humidity. Also, the analysis derived from stepwise regression, which uses on average three observations, is very highly correlated with the analysis derived from an average of 17 of the closest observations.

5.3.5 The 500-mb Wind Analyses

Finally, the OI scheme is also successful when analyzing wind fields. Table 20 shows the average errors and rms errors of the v component of wind and confirms the similarity between analyses using an average of 17 OI-1 and the analysis derived from the FSR scheme.

Table 18. The 500-mb humidity analysis errors using the OI at the observation points over the Eurasian region. The OI-1 and FSR are defined in Table 17, and FIRST GUESS is the forecast error.

	FIRST GUESS	OI-1	FSR
Average of Observed Minus Analyzed (%)	1.48	-0.02	0.17
RMS difference between Observation and the Analyses	26.6	4.61	4.6

Table 19. The average correlations among relative humidity analyses derived first from optimum interpolation of up to 20 of the closest observations (OI-1), observations and second from optimum interpolatiion of observations selected by (FSR). These analyses are also correlated with the FIRST GUESS (36-hr forecast) and observed value (OBVAL).

	OI-1	FSR	OBVAL	FIRST GUESS
OI-1	1	0.988	0.971	0.543
FSR	0.988	1	0.969	0.543
OBVAL	0.971	0.969	1	0.414
FIRST GUESS	0.543	0.543	0.414	1

Table 20. The difference between the FIRST GUESS (36-hr RWFM forecast) and the v-wind component analysis on a grid over Eurasia. The OI-1 and FSR are defined in Table 17.

	OI-1	FSR
Average Value (m/s)	1	0.91
Root Mean Square (m/s)	3.77	3.65

The accuracy of the analysis was measured by comparing an analysis made at gridpoints and interpolated to observation points to the observed value at that point. Table 21 shows that analyzed wind errors, when compared to the first guess errors, were reduced by 83 percent, which is a typical error reduction for the scheme.

Table 22 shows that the analyzed wind field is very highly correlated with the observed wind field. Also, the analysis derived from stepwise regression, which uses on average three observations,

Table 21. The 500 mb v-wind component analysis errors (m/s) using the OI at the observation points over the Eurasian region. FIRST GUESS is defined in Table 18 and OI-1 and FSR are defined in Table 17.

	FIRST GUESS	OI-1	FSR
Average of Observed Minus Analyzed (m/s)	-1.36	-0.1	-0.17
RMS Difference (m/s) Between the Observation and the Analysis	6.02	0.93	0.99

Table 22. The average correlations among analyses of the v-wind component derived first from optimum interpolation of up to 20 of the closest observations (OI-1) and second from optimum interpolation of observations selected by FSR. These analyses are also correlated with the FIRST GUESS (36-hr forecast) and OBVAL.

	OI-1	FSR	OBVAL	FIRST GUESS
OI-1	1	0.9899	0.9879	0.8935
FSR	0.9899	1	0.9876	0.8935
OBVAL	0.9879	0.9876	1	0.8720
FIRST GUESS	0.8935	0.8935	0.8720	1

is very highly correlated with the analysis derived from an average of 17 of the closest observations.

The results of experiments with the u-component of wind are virtually identical. Therefore, they offer no further insight.

6. STATUS AND PLANS

STC Task 1, development of a RAP, is nearly completed. The OI scheme, using univariate correlations and stepwise regression, has successfully analyzed all meteorological variables. All that remains is to test the scheme with multivariate correlations to determine if a better analysis is

possible. Also, the scheme will be tested to ensure that neglecting observation errors is a valid assumption in practice.

STC Task 2, calculation and modeling of the first-guess forecast errors and the OSSEs, are now the main focus of attention. All required databases have been prepared to support the error correlation module, described in Section 4.5. The RAP will test the validity of the error models on independent data sets.

STC Task 3, the RAP objective verification program, has been informally underway for several months but on a low priority basis. It will, however, be ready for operational use before Task 2 requires it. Appendix B is a detailed report on a comparison of the GSM and RWFM with the verifying analyses from HIRAS. The comparison was completed early to ensure that the forecast database, which consists of 12 nearly independent summer and winter forecasts, contained only "good" data because our sample is too small to allow the calculations of error correlations to be overwhelmed by a bad forecast.

STC Task 4, the OSSEs, began in December 1990. The observation database is complete, and the analysis and forecast databases are being developed. The subtasks detailed in Section 2.4 will be accomplished by summer 1992.

STC Task 5, extends the analysis prepared as a result of the RAP into a 12-hr forecast. This portion of the project will be started in spring 1992.

7. SUMMARY AND CONCLUSIONS

The RAP represents a unique technical approach to a regional analysis. No other group integrates the FSR into optimum interpolation to select observations rigorously for input into an optimum interpolation scheme. In addition, the scheme as developed in Eq. 2 can ignore the observation error, which is an unknown quantity, at gridpoints. This is not the typical approach to optimum (or, strictly speaking, statistical) interpolation. The optimum interpolation analysis scheme, even when using a relatively simple, univariate correlation model, performs accurate analyses of any meteorological variable.

REFERENCES

Air Force Global Weather Central, 1986: *High Resolution Analysis System (HIRAS) Tech Note.* AFGWC, Offutt Air Force Base, Nebraska.

Dey, C. H., and L. L. Morone, 1985: Evolution of the National Meteorological Center Global Data Assimilation System: January 1982-December 1983. *Mon. Wea. Rev.*, **113**, 304-317.

DiMego, G. J., 1988: The National Meteorological Center Regional Analysis System. *Mon. Wea. Rev.*, **116**, 977-1000.

Franke, R. 1990. *Sensitivity of the Error in Multivariate Statistical Interpolation to Parameter Values.* Technical Report, Naval Postgraduate School, Monterey, California.

Hoke, J. E., N. A. Phillips, G. J. DiMego, J. J. Tuccello, and J. G. Sela, 1989: The Regional Analysis and Forecasting System of the National Meteorology Center. *Wea. Forecasting*, **4**, 323-334.

Hollingsworth, A., and P. Lonnberg, 1986: The statistical structure of short-range forecast errors as determined from radiosonde data. Part I: The wind field. *Tellus*, **38**, 111-136.

Keegan, T. J., and R. Shapiro, 1985: *Methods of Meteorological Data Specification and Objective Field Analysis: A Review.* Technical Report AFGL-TR-85-0223, Air Force Geophysics Laboratory Atmospheric Sciences Division (AFGL/LYS), Hanscom Air Force Base, Massachusetts. ADA160397

Lonnberg, P., and A. Hollingsworth, 1986: The statistical structure of short-range forecast errors as determined from radiosonde data. Part II: The covariance of height and wind errors. *Tellus*, **38**, 137-161.

Mitchell, H. L., C. Charette, C. Chouinand, and B. Braslett, 1990: Revised interpolation statistics for the Canadian data assimilation procedure: Their derivation and application. *Mon. Wea. Rev.*, **118**, 1591-1614.

Redder, C. R., and N. Fukuta, 1989: Empirical equations of ice crystal growth microphysics for modeling and analysis, I. Mass and dimensions. *Atmos. Res.*, **24**, 247-272.

Schaaf, C., 1990: Finalized RAP OSSE Scenarios. Letter dated August 28, 1990, Air Force Geophysics Laboratory, Atmospheric Sciences Division (AFGL/LYA), Hanscom Air Force Base, Massachusetts.

Shapiro, R., 1978: Interpolation of data between uniform grids of differing lengths. *Mon. Wea. Rev.*, **106**, 738-745.

Shapiro, R., 1975: Linear filtering. *Mathematics of Computations*, **29**, 1094-1097.

Thiebaux, H. J., H. J. Mitchell, and D. W. Shantz, 1986: Horizontal structure of hemispheric forecast error correlations for geopotential and temperature. *Mon. Wea. Rev.*, **114**, 1048-1066.

APPENDIX A

SOFTWARE REPORT

This software report provides a brief description of problems encountered with government furnished data and operational software, a detailed listing of the required software modifications, and a short summary of the software developed for the regional analysis procedure (RAP).

1. PROBLEMS

A. DATA EXTRACTION FROM "FOREIGN" MAGNETIC TAPES

The datasets of analyses and observations from the U.S. Air Force Environmental Technology Applications Center (USAFETAC) were not user-friendly, especially the observations (surface, upper air, and satellite-measured temperatures). While the High-Resolution Analysis Model (HIRAS) analyses are fixed-length records in ASCII, the observations are variable length, unformatted records. The VAX FORTRAN language and utility programs at the Phillips Laboratory Geophysics (PL/GL) Computer Center are not well suited to read tapes generated on non-VAX hardware (that is, foreign tapes) in any event; variable length, unformatted binary records present even more problems. Nevertheless, Science and Technology Corporation (STC) developed methods to decode and process DATSAV2 surface data and DATSAV upper air data, both of which are in binary format.

A VAX consultant from the PL/GL Computer Center provided a FORTRAN subroutine, QIO_READ, which contained VAX system subroutines for extracting data from foreign tapes. These system routines, however, produced meteorological nonsense when used to extract upper air data from binary tapes. After examining the binary data from tape data dumps and converting the contents of each byte from binary to decimal format, it was apparent that reversing the order of the bytes yielded meteorological information. The IBM hardware, which USAFETAC uses, processes each byte within half or whole words in reverse order during data transfers to and from tapes. Additional programs were modified into STC subroutines FLIP_HWORD and FLIP_WWORD, to properly process each half and whole word integer produced by IBM hardware.

B. DEBUGGING THE RELOCATABLE WINDOW ANALYSIS MODEL (RWFM) FORECAST ERROR

A very large RWFM forecast error was caused by an error in the U.S. Air Force Global Weather Cental (AFGWC) software. The initial analysis and forecasts at 70 and 50 mb were much too warm; the height field was more than 5,000 m above standard! The other variables at those levels and all variables at the 100-mb level and below, however, verified well.

The cause of the forecast error was located in Subprogram RWPOST, the post-processing program of the RWFM consisting of several thousand lines of code (reference the AFGWC RWFM package/Subprogram RWPOST). Exhaustive checking of each module and debugging of those that could have caused the error isolated the problem in a section of code in Subroutine CALC01, which (for no apparent reason) recalculates the temperature at the top sigma level. Not only was the recalculation unnecessary, it was incorrect.

STC called AFGWC to advise them of the error and to eliminate it by removing the three (illogical) lines of code that recalculated the variables TSUM, PENV, and TS. (The code was located immediately above the statement, 90 CONTINUE.

C. GRID CONVERSION

The conversion from the RWFM grid to the uniform gridded data field (UGDF) grid was a deceptively "simple" task. It was expected to be simple because AFGWC had developed the software and prepared the documentation more than a year before sending it to STC; the simplicity of the task was deceptive, however, because some of the software and documentation had errors. The errors are documented thoroughly for AFGWC's information.

The requirement was to interpolate fields from the RWFM grid on a Lambert conformal (or Mercator) projection to the UGDF on a polar stereographic (or Mercator) projection. STC had followed AFGWC's lead by running the RWFM on the Lambert conformal projection for a midlatitude window. This was a sensible choice that nevertheless caused difficulties when converting to the UGDF grid.

When the latest version of software and documentation arrived from AFGWC, STC learned for the first time that the UGDF grid was defined only for polar stereographic and Mercator projections. Unfortunately, no code for interpolating a grid system on a Lambert conformal projection to a UGDF grid was provided. This problem became more complicated because the software was neither thoroughly tested (there were some obvious errors, such as a grid length that changed across the Greenwich Meridian, that testing would have revealed) nor well documented (AFGWC could not answer questions about input required by their software because the programmers were unavailable). After finding additional obscure errors in both the software and the documentation, STC determined that developing original software was the best solution to the problem. The errors, however, are documented below.

1. Reference the AFGWC/TN - 79/003 (REV), MAP PROJECTIONS AND GRID SYSTEMS FOR METEOROLOGICAL APPLICATIONS.

   a. Equation 2.11 (on page 17 in the Tech Note) describes the y-axis in an image plane coordinate system for a Mercator projection. This equation, however, is a specific version of the more general formula incorporated into the RWFM preprocessing software, and is valid only if the center point (reference) latitude (PHI0) is 0°.

      The Tech Note, however, does not refer to the generalized equation used in the RWFM software nor does it address the limitations of Eq. 2.11. Furthermore, the software documentation does not discuss the transformation equation, which can only be examined upon detailed inspection of the source code. This incomplete documentation led to erroneous software based on the assumption that Eq. 2.11 was used in the AFGWC code.

      In the derivation leading to the general form of Eq. 2.11, reference was made to code in Subroutine MERC, which sets up a Mercator grid. MERC calculates the latitude and longitude for each gridpoint. A rearrangement of terms in the section of code that calculates the latitude (contained within the DO 130 loop) yields the following expression:

      PHI = [2.0*ATAN(EXP(Y/ECOS)) -2.0*PI/4] + PHI0

where PHI is the latitude of the gridpoint, ECOS is the length of cosine side of earth radius, and Y is the y-coordinate on the grid.

This expression for PHI follows from the code

$$DEGLAT(I,J) = PHI2 + CENLTD$$

after substituting for PHI1 and PHI2, and defining PHI0 = CENLTD. From several algebraic manipulations, an expression for the y-coordinate can be solved:

$$Y = ECOS * \ln [\ TAN\ 1/2(PHI-PHI0 + PI/2)\ ].$$

Now ECOS = (A * COS[true latitude]), where A is the Earth's radius, in Subroutine MERC. Substituting the value of ECOS into the above expression for Y allows a direct comparison with Equation 2.11 of the Tech Note,

$$Y = (A*COS(PHI1)) * \ln[\ TAN\ 1/2(PHI + PI/2)\ ],$$

where PHI1 is the true latitude.

Clearly, the expressions for the y-coordinate in Subroutine MERC and Eq. 2.11 in the Tech Note are equivalent if and only if PHI = (PHI-PHI0), that is, when PHI0 = 0, which means that the center point latitude for the Mercator projection must be the Equator. Nothing in the documentation, however, required this limitation.

b. Equation 3.43 (on page 68 of the AFGWC Tech Note) calculates the latitude (PHI) of any gridpoint, given its I and J coordinates. This equation applies only to a whole mesh grid, however, because ($\Delta\lambda$), the longitudinal grid spacing in degrees is not multiplied by the grid scale factor (G) as it is in Eq. 3.44. Therefore, Eq. 3.43 yields latitudes much too large due to the larger number resulting from the calculation of (JE-J). To correct Eq. 3.43, $\Delta\lambda$ must be multiplied by the mesh scale factor G (for example, G = +0.25 for a quarter-mesh grid in the Northern

Hemisphere) prior to taking the exponential. The correct term is, then, exp [PI* G * $\Delta\lambda$/180 * (JE-J)].

2. Reference AFGWC RWFM package/Subprogram RWGRID. STC found a mistake in the mesh generation code that resulted in increased forecast errors. For the Mercator projection the true latitude was set to 30° from the center point latitude in a parameter statement in Subroutine SETGRD. But this is inconsistent with Subroutine PARAM in the DO 80 loop, which is calculating map factors for a Mercator projection. The calculation of the variable QMAP involves a "hard-wired" constant value of 0.92388. This happens to be the cosine of 22.5°, a value apparently not changed when the software was modified to set the true latitude to 30° from the center point latitude. The oversight produced an erroneous map scaling factor, which in turn affected the RWFM forecasts generating the STC database (to be used for calculating error correlations). This error in the code will be treated as a forecast error for RAP purposes.

2. SOFTWARE DEVELOPMENT

The RAP has mostly been a large software development project, consisting of five major modules. The purpose of these modules is to read the data from the magnetic tapes from USAFETAC, to build the forecast and observation databases, to perform numerical analysis experiments, to calculate forecast error correlations, and to build a database of simulated First GARP [Global Atmospheric Research Program] Global Experiment (FGGE)-2b observations for the OSSEs.

A. EXTRACTING DATA FROM FOREIGN MAGNETIC TAPES AND BUILDING THE RAP FORECAST AND OBSERVATION DATABASES

In addition to the modifications of the VAX-provided software discussed in Section 1A, programs were developed to read HIRAS, DATSAV surface observations, and DATSAV2 upper air observations (RAOB, aircraft, and satellite).

Sorting and merging all the data required development of a database management system that was reliable, flexible, and user-friendly. All data are stored on the PL/GP Computer Center's Centralized File Storage System (CFSS) for efficient retrieval and also on magnetic tape for backup. In contrast to storage on USAFETAC's tapes, the data are sorted synoptically to facilitate the calculation of forecast errors.

The primary programs are: BACKUP_CFSS.COM, which copies files from CFSS to magnetic tape; HIRASREAD.FOR, which read HIRAS from the magnetic tapes from USAFETAC/OL-A; MSC_EDIT.FOR, which selects all observing stations within a window defined by the program SETGRID.FOR; MSC_SF.FOR and MSC_UP.FOR, which create the global master station catalog for rawinsonde and surface stations, respectively; SATWRITE.FOR, which combines satellite data from several tapes onto one tape; READ_ETAC.COM, which is a command procedure for running the tape-reading jobs in batch mode; READ_VTAPE.COM, which copies files from magnetic tape to CFSS; AIRREAD.FOR, which reads aircraft data from USAFETAC tapes; SURFDREAD.FOR, which reads surface data from USAFETAC tapes; and UPPERREAD.FOR, which reads upper air data from USAFETAC tapes.

B. OPTIMUM INTERPOLATION

The optimum interpolation scheme, based on objective data selection by forward stepwise regression (FSR), has been carefully tested on all meteorological variables. This includes gross error and buddy checks, which identify observations that might be eliminated from an analysis.

The primary programs are BUDCHK.FOR, which is described in great detail in Section 3.5 of the report: EXP3.FOR, which tests the algorithm that selects observations by forward stepwise regression; EXP4.FOR (EXP5.FOR), which calculates the analyzed value at an observation (grid) point by optimum interpolation; INTRP.FOR, which maps from the RWFM's Lambert Conformal or Mercator grid to the UGDF polar stereographic or Mercator grid, respectively; SETGRID.FOR, which creates a grid and calculates the gridpoint latitude and longitude from user-defined parameters: central point,resolution, projection, and number of columns and rows; and RAPLIB.FOR, which contains a library of subroutines called by EXP3.FOR, EXP4.FOR, EXP5.FOR, and others.

C. ERROR CORRELATION CALCULATIONS

Only the general software for calculating error correlations was completed as of the writing of this report. The primary programs are COR_BIN.FOR, which "bins" all pairs of stations according to direction and distance; CORCALC.FOR, which calculates the horizontal error correlation coefficients of paired meteorological elements; CORCALC1.FOR, which calculates the correlation coefficients of paired meteorological elements; COR_CHDATA.FOR, which checks the observations obtained by COR_CHDATA.FOR for gross errors; COR_FGDATA, which reads a forecast file and calculates a first guess at an observation point by using a grid points-to-station interpolation; COR_SORT.FOR., which sorts the data for use in the program COR_CALC.FOR; COR_UPDATA.FOR, which extracts the observed values from a global synoptic data file of upper air observation; MSC_UP.COM, which creates the master rawinsonde station catalog; MSC_SF.COM, which creates the master surface station catalog; and MSC_EDIT.COM, which provides the required station pairs.

D. Observing System Simulation Experiments

Less software has been required so far compared to the above modules because PL/GP obtained packages for data extraction and unpacking of the T-106 forecasts and FGGE-2b observations. In addition, the PL/GP made the Air Force Geophysical Laboratory (AFGL) Statistical Analysis Package (ASA)P software available. So far the work has mostly consisted of making modifications to the provided software and developing scripts for the UNICOS on the CRAY-2 at Phillips Laboratory Supercomputer Center.

3. STC'S MODIFICATIONS TO THE RWFM

A. PREPARING DATABASE INPUT

STC developed a post-processor for the PL/GP Global Spectral Model (GSM) database files. The program performed two tasks. It changed the PL/GP GSM database files, dimensioned into arrays of 144*73, and made them 145*73 arrays by setting the 145th column equal to column 1. In addition, it wrote GSM database parameters in reverse order; that is, the 12th pressure level was

written first, and the first pressure level was written last to match the format the RWFM reads in the GSM database.

B. MODIFICATIONS TO THE RWGRID SUBPROGRAM

1. All occurrences of #IMAX were changed to 61.
2. All occurrences of #JMAX were changed to 61.
3. All occurrences of #KLEV were changed to 16.
4. Added Call Dropfile(0).
5. Added open statement for unit 5 card image data "GRIDIN".
6. Changed all #IGMAX to 145.
7. Changed all #JGMAX to 73.
8. Fixed open statement for opening "FIXED" file from 'UNFORMATTED' to 'FORMATTED'.
9. Compiled with cft77.
10. Linked with ldr.
11. Executed code.

This code created 2 files: CNGM and GRID.

A prerequisite to running RWGRID is a fixed field file containing a global grid of terrain heights and a global grid of surface drag coefficients. This global grid has a resolution of 2.5° x 2.5°. After using the fixed field file provided by AFGWC and receiving abnormal results, STC switched to a fixed field file from the RLAM at PL. This fixed field file required new software to read the RLAM file and reformat it as required by RWGRID.

C. MODIFICATIONS TO THE RWSFCT SUBPROGRAM

1. All occurrences of #IMAX to 61.
2. All occurrences of #JMAX to 61.
3. Added Call Dropfile(0).
4. Opened "SSMT" file (unformatted).
5. Opened "TSEA" file (unformatted).
6. Opened "GRID" file (unformatted).

7. Opened "AVGSFCT" file (unformatted).
8. Wrote a small program to convert card images of sea surface temperatures and 12-hr-old 1,000-mb temperatures into an unformatted SSMT file.
9. The 6 April 1988, 00 UTC Julian hour (177648) was added as the first card in the sea surface temperature file prior to running the program to create SSMT.
10. Fixed bug in an interpolation routine, as requested by, AFGWC.
11. Compiled with cft77.
12. Linked with ldr.
13. Executed code.

This program created two files: TSEA and VGSFCT.

D. MODIFICATIONS MADE TO THE RWANAL SUBPROGRAM

Because the first version of RWANAL had numerous errors in the code, STC implemented the latest version called RWHR00. The following changes were made to RWHR00:

1. All occurrences of #IMAX to 61.
2. All occurrences of #JMAX to 61.
3 All occurrences of #MAXPL to 12.
4 All occurrences of #KLEV to 16.
5. All occurrences of #IGMAX to 145.
6. All occurrences of #JGMAX to 73.
7. Added Call Dropfile(0).
8. Opened unit 5 "ANALIN" file for card image formatted input.
9. Opened unit 10 "CNGM" file for unformatted input.
10 Opened unit 11 "NEWCNGM" file for unformatted output.
11 Opened unit 12 "DBGS00F" file for unformatted input.
12. Opened unit 20 "GRID" file for unformatted input.
13. Opened unit 30 "SSMT" file for unformatted input.
14. Opened unit 40 "TSEA" file for unformatted input.
15. Opened unit 50 "FHR00" file for unformatted output.
16 Opened unit 60 "RESTART" file for unformatted output.
17. Opened unit 71 "PREWAM" file for unformatted input.

18. Most of the modifications were in Subroutine GETGSM.

This subroutine reads in the GSM database file created by our GSM postprocessor program. The changes made to Subroutine GETGSM were:

a. Added five new arrays (udummy, vdummy, tdummy, zdummy and rdummy). Each one of these array's dimensions were changes to (145*73).
b. The DATFLD call was commented in exchange for READ(12) udummy. There was no need to descale our GSM data for any of the fields, so the DO loop was commented out too. Instead of descaling, the DO loop was set by letting gsmdat(i) = udummy(i).
c. We repeated the procedure above (18b) for the v-wind component, but READ(12) vdummy was used to read the data.
d. Did same procedure above for temperatures, but READ(12) tdummy was used to read the data.
e. Did the same procedure above for the heights, READ(12) zdummy was used to read the data.
f. Changed all occurrences of #IMOIS to 6.
g. Repeated the (18b) procedure above for relative humidity, using READ(12) rdummy to read the data.
h. Modified first read of "SSMT" file to read the entire record (RJLHR,ARRAY), not just (RJLHR). ARRAY was basically a dummy array dimensioned to 145*73.
i. The GSM database Julian hour SRCJUL was set equal to the Julian hour found in the SSMT file because no julian hour was found in the PL/GP database.
j. Compiled with cft77.
k. Linked with ldr.
l. Executed code.

E. MODIFICATIONS MADE TO SUBPROGRAM RWBNDY

The following changes were made to the 4 January 1990 version of AFGWC's RWBNDY code, so it could be executed on the Cray-2 at the AFWL.

1. Created a CHARACTER*5 variable to store the name of the GSM verification file that will be opened.
2. Added Call Dropfile(0) as the first executable statement.
3. Opened unit 5 "BNDYIN" for card image input.
4. Opened unit 40 "FHR00" for unformatted input.
5. Opened unit 30 "GRID" for unformatted input.
6. Opened unit 20 "NEWCNGM" for unformatted input.
7. Opened unit 50 "BTEND" for unformatted output.
8. The following code was added after the assignment to FILOUT:

```
      IF(FCTIME .EQ. 6) THEN
        OFILE = 'GSMHR06'
          ELSE
      WRITE(OFILE,90) FCTIME
   90 FORMAT('GSMHR',I2)
    ENDIF
      WRITE(6,91) OFILE
   91 FORMAT('OPENING',A8,' FOR OUTPUT')
    OPEN(FILOUT,FILE=OFILE,STATUS='UNKNOWN',
     1FORM='UNFORMATTED')
```

9. Changed all occurrences of #BPTS to 5.
10. Changed all occurrences of #IMAX to 61.
11. Changed all occurrences of #JMAX to 61.
12. Changed all occurrences of #KLEV to 16.
13. Changed all occurrences of #MAXDIM to 61.
14. Changed all occurrences of #MAXPL to 12.
15. The following modifications were made to Subroutine GETGSM to read the GSM database.
    a. Added INTEGER FILGSM and PARAMETER (FILGSM = 19).
    b. Added CHARACTER*7 LITRAL
    c. Added REAL UDUMMY(145*73), VDUMMY(145*73), TDUMMY(145*73), ZDUMMY(145*73), RDUMMY(145*73)

d. Changed the data initialization of PERLIT to have 00 as its first value not 06

e. Added the following code in order to open the proper GSM database file:

```
LITRAL = 'DBGS' // PERLIT(FCINDX) // 'F'
OPEN(FILGSM,FILE=LITRAL,STATUS='UNKNOWN',
   FORM='UNFORMATTED')
WRITE(6,21) LITRAL
21   FORMAT(//,' OPENING ',A8,' FOR INPUT')
```

f. Commented out the DATFLD call and added a READ(12) udummy, where udummy was declared as a real array dimensioned to 145*73. It was unnecessary to descale the u-winds, so that code was commented out and the DO loop was set by letting GSMDAT(I) = UDUMMY(I).

g. Used a similar procedure with the v-Winds, but the real array vdummy was declared to be 145*73 and the READ(12) vdummy statement obtained the data.

h. Used same procedure with the temperatures, but the real array tdummy was declared to 145*73 and the READ(12) tdummy obtained the data.

i. Did the same for heights,with the real array zdummy declared to 145*73 and used READ(12) zdummy.

j. Did the same procedure for relative humidity but with a READ(12) rdummy statement, and the real array rdummy was dimensioned 145*73.

16. Compiled with cft77.
17. Linked with ldr.
18. Executed code.

F. MODIFICATIONS MADE TO SUBPROGRAM RWQNGM

The following changes were made to the 4 January 1990 version of RWQNGM so it could be executed at the Phillips Laboratory Supercomputer Center.

1. Added Call Dropfile(0) to main routine as the first executable statement in the program.
2. Changed all occurrences of #IMAX to 61.
3. Changed all occurrences of #JMAX to 61.
4. Changed all occurrences of #MAXD to 61.

5. Changed all occurrences of #KLEV to 16.
6. Changed all occurrences of #NBND to 5.
7. Added open statements in Subroutine AINDSK:
   a. Opened unit 5 "QNGMIN", a formatted file for card image input.
   b. Opened unit 24 "PSEUDO", an unformatted file for input.
   c. Opened unit 26 "GRID", an unformatted file for input.
   d. Opened unit 29 "QNCNGM", an unformatted file for output from RWGRID.
8. Opened unit 28 "RESTART", an unformatted file for input.
9. Opened unit 20 "BTEND", an unformatted file for input.
10. Opened unit FILFCT "FHR00", an unformatted file for input, after the FILFCT = 30 + (IPRNT -IRPT) statement; so that FILFCT would be defined prior to opening.
11. Created in Subroutine ARUN a character*5 variable called OFILE;, then after the declaration of FILFCT, added the following code to create unique filenames for each forecast hour:

```
      IF(ITIME .LT. 10) THEN
         WRITE (OFILE,62) ITIME
   62 FORMAT ('FHR0',I1)
            ELSE
         WRITE (OFILE,63) OFILE
   63 FORMAT ('FHR',I2)
      ENDIF
         WRITE (6,64) OFILE,ITIME
   64 FORMAT ('**** OPENING FORECAST FILE',A8,'
     1 FOR ',I2,' Hr FORECAST ')
      OPEN (FILFCT,FILE=OFILE,STATUS='NEW', FORM='UNFORMATTED')
```

12. Compiled with cft77.
13. Linked with ldr.
14. Executed code.

APPENDIX B

COMPARISON OF THE RWFM AND GSM WITH HIRAS

As part of the regional analysis procedure (RAP) quality control program, Science and Technology Corporation completed careful objective and subjective analyses of the 36-hr forecasts by the Air Force Global Weather Central (AFGWC) Global Spectral Model (GSM) and the Relocatable Window Forecast Model (RWFM). In two windows, one including Eurasia and the other Central America and southern North America, 12 surface and 500-mb forecasts at 60-hr intervals in July 1988 and January 1989 were chosen for analysis. Part I is a discussion the subjective analysis, which is based mostly on root-mean-square (rms) errors, and Part II is a discussion of the objective analyses.

In general the GSM is a slightly better model but not significantly better. At some locations on some occasions the RWFM made better forecasts; however, in the final analysis STC could not make a case for using the RWFM.

PART I. A COMPARISON OF RWFM AND GSM ERRORS

The GSM 36-hr Eurasian January mass field forecasts provide consistently smaller rms errors than the RWFM. The GSM temperature forecasts have rms errors between 0.5 and 1.5° K smaller at all levels for all cases. The GSM height forecast rms errors range from 10 to 50 m smaller than the RWFM between the 1,000- and 500-mb levels and 50 to 100 m smaller between the 100- and 50-mb levels for all cases. The GSM sea level pressure rms errors are 1 to 3 mb smaller for all cases except 00 UTC 1-6-89 (0.3 mb larger), 00 UTC 1-11-89 (0.3 mb larger), and 00 UTC 1-26-89 (1.0 mb larger). The GSM relative humidity rms errors are generally 5 to 10 percent smaller at most levels for all cases. The RWFM and GSM wind forecast rms errors are of similar quality, especially the v component of the wind vector. (From here on, u component refers to the component of the west-to-east wind vector, and similarly the v component refers to the south-to-north component of the wind vector.) The GSM u-component rms errors are 0.5 to 1.5 m/s smaller at most levels in most cases, but the RWFM had v-component rms errors at least equal to those of the GSM in 9 of the 12 cases.

The GSM 36 hr Eurasian July forecasts provide height rms errors which are 5 to 10 m smaller at most levels in all cases. The differences between the RWFM and GSM temperature rms errors are very small except at the 70- and 50-mb levels where the RWFM rms errors are 0.5 to 1.0 K smaller in every case. The GSM sea level pressure rms errors are about 1 mb smaller than the RWFM in every case except 12 UTC 1-3-89 (0.1 mb smaller). The GSM relative humidity rms errors are 1 to 5 percent smaller at most levels in most of the cases. The RWFM u component and v component rms errors are 0.5 - 1.5 m/s smaller than the GSM at almost all levels for all the cases.

The RWFM and GSM 36 hr Central American January rms errors of the mass field forecast are similar. The RWFM and GSM height and temperature rms errors are similar up to the 100-mb level, above which the RWFM errors are about 10 m and 0.5 K smaller for almost all the cases. The GSM sea level pressure rms errors are 0.2 - 0.5 mb smaller than the RWFM for all cases except 12 UTC 1-3-89 (1.3 mb smaller) and 00 UTC 1-26-89 (0.8 mb smaller). The RWFM and GSM relative humidity rms errors are within 1 to 3 percent of each other at all levels for almost all the cases. The RWFM and GSM momentum field rms errors are similar except between 500 and 200 mb, where the GSM u component and v component rms errors are 0.5 - 2.0 m/s smaller than the RWFM for almost all the cases.

The RWFM 36 hr Central American July height, temperature, and relative humidity forecasts provide rms errors that are equal to or smaller than the GSM at most levels in every case. The RWFM temperature rms errors are 0.5 to 1.5 K smaller than the GSM between 100 and 50 mb in every case. The RWFM height rms errors are 5 to 10 m smaller than the GSM between 300 and 50 mb in most cases. The GSM sea level pressure rms errors are 0.1 to 0.3 mb lower than the RWFM in all cases except 00 UTC 7-1-88 (equal), 00 UTC 7-6-88 (0.1 mb larger), 00 UTC 7-11-88 (O.4 mb larger), and 00 UTC 7-26-88 (equal). The RWFM and GSM relative humidity rms errors are within 1 to 3 percent at all levels for every case. The RWFM u component and v component rms errors are 0.5 to 1.0 m/s smaller than those of the GSM in most cases, especially between 1,000 and 200 mb.

PART II. AN OBJECTIVE COMPARISON OF THE 36-HR FORECASTS BY THE RWFM AND GSM TO THE VERIFYING ANALYSES BY THE HIGH RESOLUTION ANALYSIS SYSTEM (HIRAS) MODEL

00 UTC 1-1: The RWFM and GSM failed to dig a strong short wave trough and to intensify the associated 959 mb surface low north of Norway by 9 and 11 mb, respectively. The RWFM underdeveloped the western Eurasia surface high by 12 mb, while the GSM underdeveloped it by 5 mb.

12 UTC 1-3: The RWFM failed to develop the cutoff low in the northeastern portion of the long wave trough over the Soviet Union. Both the RWFM and GSM failed to develop the closed 1,000-mb surface low southward towards the Caspian Sea; the RWFM forecast a 987-mb low 600 miles to the northwest where HIRAS had analyzed a 1,012-mb high, and the GSM forecast a 994-mb low about 200 miles northwest of where HIRAS had analyzed the low. The RWFM underdeveloped the 1,038-mb surface high over Greece by 10 mb.

00 UTC 1-6: The GSM intensity and position forecasts of the 988 mb Iceland and 982 mb northern Soviet Union surface lows were much better than the RWFM, which underforecast these lows by 4 and 6 mb, respectively. The RWFM and GSM underforecast the 500 mb cutoff low over the Barents Sea by 140 and 80 m, respectively. The RWFM underintensifies the associated 982 mb surface low by 6 mb while the GSM intensity matched the HIRAS.

12 UTC 1-8: The RWFM overintensifies the 980 mb Scandinavian surface low by 7 mb while the GSM matched the HIRAS intensity. Both the RWFM and GSM underdeveloped the 1,040-mb surface high over the eastern Soviet Union by 8 and 10 mb, respectively. The RWFM and GSM overintensified The 1,028-mb trough east of the Caspian Sea by 10 and 9 mb, respectively.

00 UTC 1-11: The GSM overintensified the northern Soviet Union 988-mb surface low by 7 mb. Both the RWFM and GSM overintensified the 968 mb Iceland surface low by 7 mb and underdeveloped the 1,034-mb Yugoslavian surface high by 4 and 5 mb, respectively. The RWFM underforecast the depth of the 500 mb Barents Sea trough by 60 m while the GSM matched the HIRAS intensity.

12 UTC 1-13: Both models failed to dig the strong 500 mb short wave trough into Turkey, where heights were forecast 140 m too high. Both the RWFM and GSM underforecast the associated 1,018 mb surface low over the eastern Mediterranean Sea by 3 and 6 mb, respectively. Both models failed to cut off the 500-mb low over the northern Soviet Union, although the GSM deepened the trough more than the RWFM. The RWFM and GSM underdeveloped the 1,026 mb surface high over the northern Soviet Union by 7 and 5 mb, respectively. The RWFM underdeveloped the 1,040 mb western Europe surface high by 4 mb. The RWFM underforecast the 955 mb Iceland surface low by 7 mb while the GSM overintensified it by only 1 mb.

00 UTC 1-16: The RWFM underdeveloped the 500-mb high and its associated 1,034 mb surface high over the Mediterranean Sea by 80 m and 6 mb, respectively. Both the RWFM and GSM failed to intensify the 500 mb short wave trough over Finland and incorrectly phased it with Caspian Sea trough. The RWFM underforecast the Finland 976 mb surface low by only 1 mb, but the low is elongated towards the southeast and not as circular as the HIRAS low, due to incorrect phasing of the system with the Caspian Sea low. The GSM underforecast this system by 7 mb and suffered the same phasing problem as the RWFM.

12 UTC 1-18: The RWFM deepened the 500-mb low too much over the southern Soviet Union by 60 m and overintensified the associated 1,005 mb surface low by 13 mb. The GSM correctly maintained the positive tilt and intensity of the southern Soviet Union 500-mb trough but overintensified the surface low by 7 mb. Both the RWFM and GSM overintensified the 972 mb surface low over the Arctic Ocean by 14 and 16 mb, respectively, but the forecast position of the GSM is closer to HIRAS than that of the RWFM. The RWFM underdevelops the 1,037 mb surface high over southern Europe by 9 mb. Both the RWFM and GSM underdeveloped the 1,040 mb surface high over Siberia by 11 and 16 mb, respectively.

00 UTC 1-21: The RWFM overintensified the 500-mb low and its associated 1,016 mb surface low over Iraq by 50 m and 7 mb, respectively. The RWFM underdeveloped the trough over the Soviet Union by 60 m.

12 UTC 1-23: The RWFM and GSM underforecast the Greenland 500-mb trough by 150 m. The GSM failed to develop the 500 mb short wave ridge and the associated 1,036 mb surface high over Siberia. The RWFM and GSM incorrectly developed individual 500 mb cutoff lows instead

of splitting the 500-mb trough west of the Siberian high into an open short wave trough and a cutoff low. The RWFM and GSM placed the associated 992 mb surface low about 500 miles northwest of the HIRAS analyzed position with intensities of 989 and 993 mb, respectively. The RWFM and GSM placed the 1,038 mb European surface high about 500 miles west of the HIRAS position with intensities of 1,037 and 1,035 mb, respectively. The RWFM underforecast the 975 mb Arctic Ocean surface low by 10 mb and placed it about 300 miles south of the position analyzed by HIRAS. The GSM underforecast this low by only 3 mb and placed it very close to the HIRAS position.

00 UTC 1-26: The RWFM underforecast the Soviet Union trough by 60 m. The GSM overintensified the 1,008 mb surface low over northern Siberia by 15 mb and the 977 mb surface low over the Barents Sea by 6 mb, while the intensities of these lows forecast by the RWFM are within 2 mb of HIRAS. The RWFM and GSM underdeveloped the Eurasian surface high by 3 and 5 mb, respectively,and both the RWFM and GSM underdeveloped the 952 mb Iceland low by 12 mb.

12 UTC 1-28: The RWFM and GSM overintensified the 955 mb Arctic low by 13 and 16 mb, respectively. The RWFM failed to build the 1,045-mb surface high across Europe.

CENTRAL AMERICAN WINDOW IN JANUARY 1989

00 UTC 1-1: The RWFM and GSM failed to develop the 1007 mb closed surface low off the mid-Atlantic coast, as both models forecast open troughs. Both the RWFM and GSM underforecast the 1,006-mb surface low over South America by 5 and 6 mb, respectively, with the RWFM position 400 miles too far south and the GSM position 200 miles too far east.

12 UTC 1-3: The RWFM placed the 500-mb trough south of Nova Scotia 300 miles to the west of the HIRAS-analyzed position. This placement could explain the 15 mb underintensification of the associated 964 mb surface low; however, the RWFM position of the surface low is very close to the HIRAS position. The GSM forecast intensity of the surface low matched the intensity analyzed by HIRAS, but the low's position is about 200 miles west of the HIRAS position. The RWFM and GSM underforecast the 500-mb low over Central America by 30 and 40 m, respectively. The RWFM and GSM underdeveloped the 500-mb high over Mexico by 50 and 20 m, respectively. The RWFM and GSM underforecast the 1,005 mb surface low over South America by 7 mb.

00 UTC 1-6: Both the RWFM and GSM failed to develop the weak 500 mb short wave trough and the closed 1,017 mb surface low off the mid-Atlantic coast, developing weak surface troughs instead. The GSM showed more evidence of the weak 500-mb trough than the RWFM.

12 UTC 1-8: The GSM closed off the 500-mb high over the Bahamas but underdeveloped it by 20 m, while the RWFM placed it too far east without closing it off. The RWFM deepened the 500-mb trough too far into Mexico with a subsequent southward displacement of the surface high.

00 UTC 1-11: The RWFM and GSM failed to develop the weak surface trough east of the Bahamas. The RWFM correctly developed the weak mid-Atlantic coastal trough while the GSM failed to develop it.

12 UTC 1-13: The RWFM underdeveloped the 1,036 mb Atlantic surface high by 3 mb but correctly developed the mid-Atlantic coastal trough, which the GSM did not develop. The RWFM underforecast the midwestern 500 mb short wave trough. Both the RWFM and GSM underforecast the Central American surface low by only 3 mb, but they underdeveloped the South American surface low by 5 and 7 mb, respectively.

00 UTC 1-16: The RWFM underforecast the 1,004 mb Great Lakes surface low by 4 mb.

12 UTC 1-18: Both the RWFM and GSM underforecast the HIRAS-analyzed 500 mb short wave trough and its associated 996 mb surface low off the U.S. east coast: the GSM forecast a closed 1,003-mb low and the RWFM an open 1,004-mb low. The RWFM and GSM failed to develop the 500 mb cutoff lows south of Central America, forecasting heights 60 m high instead. The RWFM and GSM underforecast the Central American 1,005 and 1,004 mb surface lows by 6 mb and South American surface lows by 4 mb.

00 UTC 1-21: The RWFM underforecast the gulf coast 500 mb trough and associated surface trough, resulting in an underforecast onshore flow along the southeast coast. The GSM forecast this system much better.

12 UTC 1-23: The RWFM and GSM underforecast the 500 mb short wave trough and the associated 1,006 mb surface low off the U.S. east coast by 5 and 8 mb, respectively.

00 UTC 1-26: The RWFM and GSM failed to develop the weak 500 mb short wave trough over the upper midwestern U.S.

12 UTC 1-28: The RWFM and GSM underforecast the closed surface lows in Central America and South America by 5 to 7 mb.

EURASIAN WINDOW IN JULY 1988

00 UTC 7-1: Both the RWFM and GSM overintensified the 500-mb trough over Turkey by 40 m. The RWFM and GSM overintensified the 1,004 mb surface low over the northern Soviet Union by 4 and 6 mb, respectively.

12 UTC 7-3: The GSM underforecast the Great Britain 500 mb cutoff low by 60 m and the associated 996 mb surface low by 5 mb, but the RWFM forecast of this system matched the HIRAS analysis. Both forecast models underforecast the Arctic Ocean 500 mb cutoff low by 60 m and the 990 mb Iranian surface low by 14 mb.

00 UTC 7-6: The RWFM and GSM underforecast the 500-mb high over Sicily by 70 and 30 m, respectively.

12 UTC 7-8: HIRAS is missing.

00 UTC 7-11: The RWFM and GSM underdeveloped the 500-mb high over the Soviet Union by 70 and 40 m, respectively. The RWFM and GSM overintensified the 1,008-mb surface trough over the Caspian Sea by 7 and 4 mb, respectively. The RWFM and GSM overintensified the 1,008 mb Arctic trough north of the Soviet Union by 8 and 3 mb, respectively.

12 UTC 7-13: The RWFM and GSM underforecast the 500-mb trough over the Caspian Sea by 40 m. Both models underforecast the 993 mb surface low over Iran by 10 mb. The RWFM and GSM overintensified the 1,008 mb Arctic Ocean low by 6 and 5 mb, respectively, and the 1,012 mb Greenland surface low by 3 and 5 mb, respectively.

00 UTC 7-16: The RWFM and GSM underforecast the 1,004 mb surface low over the northern Soviet Union by 6 and 4 mb, respectively, and forecast a 1,012 mb surface high over Afghanistan, where HIRAS has a 996 mb surface trough.

12 UTC 7-18: The RWFM and GSM underforecast the intensity of the dual 500 mb cutoff low over northern Siberia and the Arctic Ocean by 90 and 40 m, respectively. The RWFM underforecast the associated 995 mb surface low by 6 mb, while the GSM overintensified it by only 1 mb. The RWFM and GSM underforecast the 996 mb Iceland surface low by 4 mb and the 1,006 mb Scandinavian surface low by 8 mb. Both models overdeveloped the European surface high by 4 mb and the southern Soviet Union surface high by 10 mb.

00 UTC 7-21: The RWFM underforecast the 500 mb cutoff low over northern Siberia by 120 m and the associated 994 mb surface low by 13 mb. The GSM underforecast this 500-mb low by only 20 m and the surface low by only 1 mb, but the GSM placed the surface low about 500 miles northwest of the HIRAS position. The GSM overintensified the surface low over the North Sea by 6 mb, while the RWFM underforecast it by 4 mb. Both the RWFM and GSM underdeveloped the 500-mb high over Iran by 100 m and underforecast the 996 mb surface low over Afghanistan by 8 mb.

12 UTC 7-23: The RWFM and GSM underforecast the 500 mb cutoff low over northern Siberia by 160 and 80 m, respectively, with the RWFM failing to cut it off. The RWFM and GSM underforecast the associated surface low by 8 and 4 mb, respectively. The RWFM and GSM underforecast the 984 mb Icelandic surface low by 7 and 4 mb, respectively.

00 UTC 7-26: The RWFM and GSM underforecast the 500-mb high over Afghanistan by 100 m. The RWFM and GSM underforecast the 500-mb low over the Soviet Union by 30 and 50 m, respectively. The RWFM and GSM underforecast the 996-mb low over Afghanistan by 8 mb.

12 UTC 7-28: The RWFM and GSM underforecast the 500 mb cutoff low over northern Siberia by 120 and 20 m, respectively. The RWFM and GSM underforecast the 500 mb cutoff low over the Soviet Union by 60 and 40 m, respectively. The RWFM and GSM underforecast the Arctic Ocean 1,026 mb surface high by 4 and 5 mb, respectively.

CENTRAL AMERICAN WINDOW IN JULY 1988

00 UTC 7-1: The RWFM and GSM forecast the New England 500 mb short wave trough about 200 miles west of the position analyzed by HIRAS. The RWFM and GSM underforecast this trough by 60 and 30 m, respectively. Both models underforecast the broad South American surface low by 4 to 6 mb.

12 UTC 7-3: Both the RWFM and GSM underforecast the 500 mb cutoff low over South America by 80 m. The RWFM underforecast the Central American surface low by 4 mb. The RWFM and GSM underforecast the South American closed surface low by 5 and 7 mb, respectively. Both models underforecast the surface trough over the Bahamas by 3 mb.

00 UTC 7-6: Both the RWFM and GSM failed to develop the weak 500-mb trough off the U.S. east coast, although the GSM hinted at more development than the RWFM. Both models underdeveloped the 500 mb Bermuda high by 40 km and the associated 1,032 mb surface high by 8 mb.

12 UTC 7-8: HIRAS is missing.

00 UTC 7-11: Both the RWFM and GSM underforecast the South American 500 mb cutoff low by 110 m and the associated 1,012 mb surface low by 4 mb. The RWFM underforecast the closed 1,011 mb surface low over southern Mexico by 4 mb, while the GSM overintensified this low by 4 mb.

12 UTC 7-13: Both the RWFM and GSM underforecast the broad area of low 500-mb heights south of 10° north by 40 to 80 m. Both models underforecast the Montana surface low by 9 mb and the Central American surface low by 4 mb.

00 UTC 7-16: Both the RWFM and GSM underforecast the 1,028 mb surface Bermuda high by 4 mb. Both models underforecast the relatively low 500-mb heights south of 10° north latitude by about 50 m.

12 UTC 7-18: Both the RWFM and GSM failed to forecast the closed 500-mb low over the southern Gulf of Mexico, missing the intensity by 100 m. The RWFM and GSM underforecast the 1,032 mb surface Bermuda high by 7 and 6 mb, respectively. Both models underforecast the 1,011 mb Central American closed surface low by 4 mb and the 1,010 mb Brazilian closed surface low by 6 mb.

00 UTC 7-21: Both the RWFM and GSM underforecast the midwestern U.S. 500-mb trough by 30 m and the Central American surface low by 5 mb. Both models underforecast the surface Bermuda high by 6 mb.

12 UTC 7-23: Both the RWFM and GSM underforecast the eastern U.S. 500-mb trough by 30 m. The RWFM failed to develop the 1,015 mb surface trough over New England, while the GSM underforecast it by 4 mb. Both models underforecast the 1,008 mb Mexican closed surface low by 8 mb and the 1,011 mb Panama closed surface low by 4 mb.

00 UTC 7-26: Both the RWFM and GSM underforecast the relatively low 500-mb heights south of 10° north by 40 m. The RWFM and GSM underforecast the 1,011 mb southern Mexico closed surface low by 5 mb and the 1,009 mb Central American closed surface low by 5 and 3 mb, respectively.

12 UTC 7-28: Both the RWFM and GSM underforecast the depth of the trough over the Canadian Maritimes trough by 30 m.

Overall, the GSM provides noticeably smaller rms forecast errors than the RWFM for active weather cases (i.e., the Eurasian and Central American winter cases), while the RWFM provides smaller rms forecast errors for relatively inactive weather cases (i.e., the Eurasian and Central American summer cases).

APPENDIX C

LIST OF ACRONYMS

AIREPS	aircraft reports
AFGL	Air Force Geophysics Laboratory (now called PL/GP)
AFGWC	Air Force Global Weather Central
ASAP	AFGL Statistical Analysis Package
ASCII	American Standard Code for Information Interchange
CA	Central America
DATSAV2	Datasave 2
ECMWF	European Center for Medium-Range Weather Forecasts
EU	Eurasia
FSR	forward stepwise regression
FGGE	First GARP Global Program
GARP	Global Atmospheric Research Program
GDA	global data assimilation
GSM	Global Spectral Model
HIRAS	High Resolution Analysis System
NMI	nonlinear mode initialization
OI	optimum interpolation
OI-1	OI analysis prepared using the 20 closest observations
OI-2	OI analysis prepared using a subset of the observations (chosen by FSR) used in OI-1
OSSE	Observing System Simulation Experiment
PL	Phillips Laboratory

PL/GP	Phillips Laboratory Geophysics Directorate
PLSC	Phillips Laboratory Supercomputer Center
RAOB	rawinsonde observation
RAP	Regional Analysis Procedure
RLAM	Relocatable Limited Area Model
rms	root mean square
RWAM	Relocatable Window Analysis Model
RWFM	Relocatable Window Forecast Model
RWFMVER	Relocatable Window Forecast Model Verification
SOAR	second order autoregressive
STC	Science and Technology Corporation
UGDF	uniform gridded data field
UTC	Universal Time Constant